ELSEVIER

Journal of Volcanology and Geothermal Research 64 (1995) 23–52

Journal of volcanology and geothermal research

Inner structure of the Krakatau volcanic complex (Indonesia) from gravity and bathymetry data

Christine Deplus[a], Sylvain Bonvalot[b], Darharta Dahrin[a], Michel Diament[a], Hery Harjono[c], Jacques Dubois[a]

[a]*Laboratoire de Gravimétrie et Géodynamique, Institut de Physique du Globe de Paris, 4 Place Jussieu, 75252 Paris, France*
[b]*Laboratoire de Géophysique, ORSTOM, 72 route d'Aulnay, 93140 Bondy, France*
[c]*Geoteknologi LIPI, Jl Cisitu, Bandung, Indonesia*

Received 30 April 1993; accepted 12 May 1994

Abstract

On 27 August 1883, the Krakatau volcanic complex (Indonesia) was the site of one of the most destructive historical eruptions. Most of the volcano was destroyed and a new caldera also formed during this catastrophic event. Since the date of the eruption, many geological studies of the superficial structures and eruption products have been carried out. A debate on the scenario of the eruption and the way the volcano collapsed has developed and still is unresolved.

In order to assess the inner structure of the volcanic complex, we carried out a detailed land and marine geophysical survey in the summer 1990. In this paper, bathymetry and gravity data collected during the survey as well as literature data are compiled and analysed. Bathymetric data show that the caldera is characterized by a flat seabottom at 240 m below sea level and by steep linear walls suggesting that the caldera collapse has been controlled by pre-existing features. Moreover, the build-up of the young active volcano, Anak Krakatau, on the very edge of the caldera could lead to mechanically unstable conditions which must be considered for hazard mitigation. The Bouguer anomaly of the volcanic complex is characteristic of volcanoes with an explosive behaviour. 3-D gravity modelling reveals the previously unknown geometry of the dense substratum of the proto-Krakatau and evidences the presence of a collapsed structure beneath the caldera filled up with low-density material.

Finally, we point out a major weakness zone, oriented N150° on a line passing through the old and recent vents of the volcano. This zone could have guided both the development of the volcanic activity and the emplacement of the 1883 caldera. Furthermore, this weakness zone passing through the summit line of the pre-1883 Krakatau volcano has been introduced as a significant disruption surface of the volcanic edifice in the updated scenario of the 1883 eruption that we propose.

1. Introduction

The Krakatau volcano, located in the Sunda Strait (Indonesia), is famous for its 1883 eruption which was one of the largest volcanic events in historic time. Although this eruption has been discussed by many authors mainly on the basis of geological investigations, only few geophysical studies were carried out on the Krakatau volcanic complex in order to constrain the inner structure of the volcano. Furthermore, the 1883 eruption resulted in the formation of a large submarine caldera which was selected by Williams (1941) as the type example of a collapse caldera:

0377-0273/95/$09.50
SSDI 0377-0273(94)00038-I

"*as the type of a caldera produced by collapse following the evisceration of a magma chamber by explosions of pumice, it seems best to select that of Krakatau, both because of the recency of its origin and the clarity of the evidence*". However, the more recent bathymetric map of the 1883 caldera has been mainly established with data collected by Escher in 1919.

In order to detail the morphology of the 1883 caldera and to better constrain the deep structure of the volcanic complex, we carried out a geophysical survey in the summer of 1990. This study is part of a French–Indonesian programme devoted to the geodynamics of the Sunda Strait (see Diament et al., 1990 for earlier studies). Our survey involves a part of an oceanographic cruise and land data acquisition on the islands of the volcanic complex. New bathymetric data were collected over the Krakatau caldera and around the islands. Side-scan sonar and

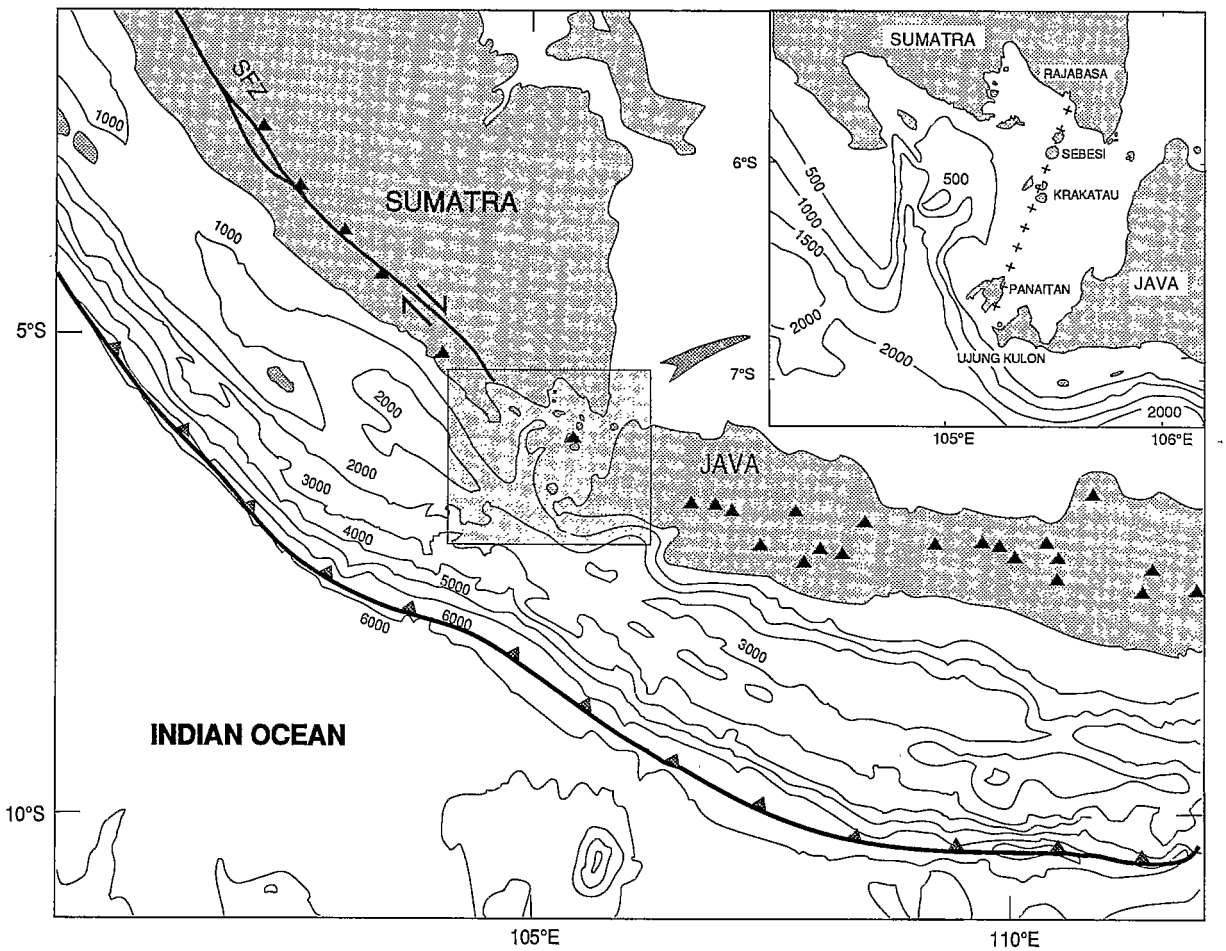

Fig. 1. Geodynamical context of the Krakatau volcanic complex. (a) Heavy solid line with black triangles=trench axis for the subduction of the Indo-Australian plate beneath the South-East Asian plate; light solid lines=isobaths in meters; black triangles=volcanoes distributed along the volcanic arc (Java and Sumatra) related to the subduction; *SFZ*=Sumatra Fault Zone. (b) Detailed view of the Sunda Strait showing the location of the Krakatau complex on a N20° volcanic line extending from Mount Rajabasa to Panaïtan island.

high-resolution seismic profiles were also recorded on some selected traverses. In addition, we realized 148 gravity measurements on the islands of the complex and about 30 magnetotelluric soundings in the audio-frequency range (8 Hz–23 kHz) and 4 in the low-frequency range (less than 0.25 Hz).

This paper presents the new bathymetry and gravity data collected during our survey. Bathymetry data analysis allows us to better constrain the present morphology of the 1883 caldera and to discuss the location of Anak Krakatau, the presently active center of the volcanic complex, on the edge of the caldera. Moreover, bathymetry combined with previous topographic mapping provide a numerical model of altitude for the reduction of gravity data. A model of the deep structure of the volcano is then proposed from gravity data modelling and is discussed in light of the historical development of the complex.

2. Geodynamical context

The Krakatau volcanic complex lies in the Sunda Strait (Indonesia) between Java and Sumatra islands and belongs to the volcanic arc related to the subduction of the Indo-Australian plate beneath the South-East Asian plate (Fig. 1). Petrologic studies have shown that Krakatau differs from the common pattern of volcanoes in Indonesia. Indeed, the eruptions cycles evolve from basaltic to dacitic composition (van Bemmelen, 1941; Zen and Sudradjat, 1983; Camus et al., 1987). The Krakatau volcanic complex is also located on a N20° volcanic line which extends across the Sunda Strait from Panaïtan island in the south to Mount Rajabasa in the north passing through Sebesi and Sebuku islands (Fig. 1). This line is outlined by shallow seismicity as revealed by world-wide seismological data (Harjono et al., 1991). The volcanic activity along this line is supposed to be recent (Nishimura et al., 1986) although there is no precise dating except on Krakatau. Presently, the Krakatau is the only active volcano of this line and displays significant seismicity which has been found to be of tectonic origin (Harjono et al., 1991). The tectonic setting of the Sunda Strait is governed by an extensional regime according to the results of recent geological and geophysical investigations (Lassal et al., 1989; Diament et al., 1990; Harjono et al., 1991).

3. Volcanic activity of Krakatau

The geological map of the Krakatau volcanic complex (from Effendi et al., 1986) is shown on Fig. 2. The complex consists in four islands (Sertung, Panjang, Rakata and Anak Krakatau). This configuration results from at least two historical destructive eruptions and from the recent emergence of Anak Krakatau. History of the volcanic activity of Krakatau can be divided into three main periods:

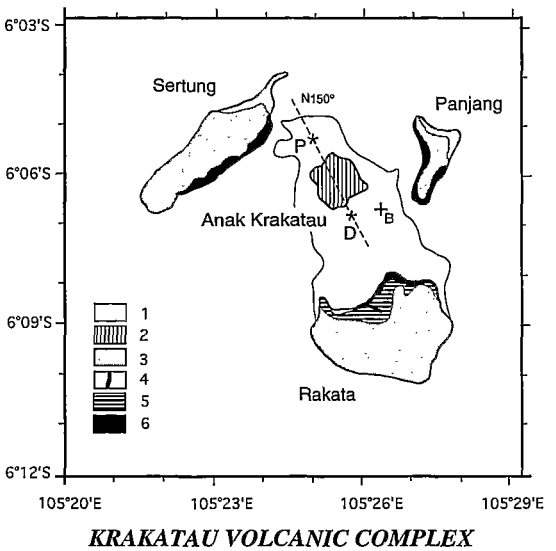

Fig. 2. Geological sketch map of the Krakatau volcanic complex (from Geological Survey of Indonesia). *1*=alluvial deposits; *2*=recent volcanic products of Anak Krakatau (basalt and andesite); *3*=pyroclastic deposits of the 1883 eruption; *4*=Rakata basaltic dyke (latest volcanic activity of Rakata); *5*=Rakata basaltic rocks; *6*=old volcanic substratum of the proto-Krakatau (trydimite andesite). *B*=Bootmans rock. Light solid line indicates the coastline of the Krakatau island before the 1883 eruption: *P*=Perbuatan crater, *D*=Danan crater. Note that the old vents (P and D) and the new one (Anak Krakatau) are distributed along a line trending N150°E.

Stage 1: Formation of a shield volcano (*Proto-Krakatau*) about 2000 m high and 10–12 km in diameter according to Verbeek (1885) and Escher (1919). Destruction of the primitive volcano would have resulted in the formation of a large sub-marine caldera which diameter is approximately 7 km. The islands of Sertung and Panjang and the basement of Rakata are remnants of the rim of this caldera. The destruction occurred about 60,000 years ago according to Ninkovich (1979) on the basis of drilling data or only 1500 to 1700 years ago according to Judd (1889) from historical documents.

Stage 2: Formation of a basaltic cone, 800 m high, on the edge of the *prehistoric caldera* and covering the Rakata remnant. Then, growth of two andesitic cones, Danan (450 m above sea-level) and Perbuatan (120 meters a.s.l.), within the caldera. These three overlapping volcanoes merged into one elongated volcanic island, Krakatau. The Krakatau island largely disappeared on 27 August 1883, leaving only half the cone of Rakata and a small rock pinnacle, Bootmans rock, exposed above sea level. The associated events were: emission of a huge volume of ignimbrite that covered the islands and the surrounding sea-floor, formation of a submarine caldera and generation of large tsunamis that killed more than 36, 000 persons on the neighbouring coastlines. Pyroclastic deposits have greatly increased the area of the islands of Sertung and Panjang.

Stage 3: Emergence of Anak Krakatau (*Child of Krakatau* in Indonesian) on January, 1928. A tuff ring (basic andesite) was constructed up to 152 m above sea level until 1959 (Sudrajat, 1982). Then, the volcanic activity migrated southwestward and built a still active cone to an height of 200 m a.s.l.. The last eruption, that began on 7 November 1992, consisted mostly of basaltic andesite lava flows (Bulletin of the Global Volcanism Network, 1992).

3.1. The 1883 eruption

Several scenarios have been proposed for the 1883 eruption (Verbeek, 1885; Stehn, 1929; Williams, 1941; Self and Rampino, 1981; Yokoyama, 1981; Camus and Vincent, 1983a,b; Francis and Self, 1983; Sigurdsson et al., 1991a). The chronology of the different events and the origin of the tsunami (Latter, 1981; Francis, 1985; Vincent et Camus, 1986; Yokoyama, 1987) have been recently largely debated in the scientific community.

The eruption can be divided into two stages on the basis of the nature and sequence of the deposits: a plinian phase followed by several large explosions and emission of a large volume of ignimbrite. It has been proposed that the caldera collapsed late in the eruption sequence subsequently to the emptiness of the magma chamber. The main differences between the two recent scenarios deal with the chronology and the way the volcano collapsed.

(1) In the first model (Self and Rampino, 1981; Francis and Self, 1983; Sigurdsson et al., 1991a,b), the culminating event was the generation of pyroclastic flows by gravitational collapse of the eruption column. Then, most of the Krakatau island disappeared into the sea when the roof of the magma chamber collapsed. Thus, the large volume of ignimbrite was erupted before major collapse of the volcano. The new caldera was formed within the prehistoric one. The authors also proposed that the tsunami were produced when the pyroclastic flows entered the sea.

(2) In the second model, Camus and Vincent (1983a,b) proposed a Mount St. Helens type collapse of the pre-existing volcano that produced a debris flow oriented towards the north and northeast (note that the collapse of Rakata would have followed the boundary of the *prehistoric caldera*). After this catastrophic event, extensive sub-marine eruption of ignimbrite took place ending with the collapse of a new caldera. According to these authors, the 1883 caldera would be located northwest of Rakata and intersects the prehistoric one. In this model the giant landslide would be responsible for the major tsunami.

These models were proposed on the basis of field geological investigations and only few geophysical studies were performed on this volcanic complex concerning its inner structure.

4. Previous geophysical studies

4.1. Gravity data

The first geophysical study was based on land gravity data gathered in 1969 and 1982 (Yokoyama and Hadikusumo, 1969; Yokoyama, 1981, 1987) on the shores of the Krakatau islands. Data reduction revealed a centrosymetric Bouguer anomaly: its maximum amplitude is circular and runs over the external islands of the complex while the minimum is centered over the bathymetric depression to the West of Anak Krakatau. However, it can be noticed that the shape and amplitude of the Bouguer anomaly is not well constrained due to the limited number of land data and to the lack of marine gravity data. The relative minimum is estimated by interpolation to be about 9 mGal. It was interpreted by Yokoyama (1981) in terms of caldera deposits which have a negative density contrast of -0.3 g/cm^3 with the basement rocks and he proposed a funnel-shape model of 4 km radius and 1 km depth. He also suggested that this low-density infill might be material which was ejected and fallen back into an explosion crater and probably consists of pumice, ash and rocks of the old volcano.

Yokoyama (1981) has then proposed that the most important factor in the disappearance of two-thirds of the Krakatau island during the 1883 eruption was a large explosion. This was later discussed by Self and Rampino (1982) and Scandone (1990) who argued that the eruption was not of the type to eject a large amount of lithic material explosively, sufficient to cause a 4–5-km diameter caldera.

Instead of an explosive event, a more likely mechanism was proposed by Verbeek as early as 1885. This mechanism leads to the disappearance of the missing part of the volcano by engulfment into a collapsed caldera. In a review paper, McBirney (1990) mentioned that such an explanation was already proposed by Fouqué in 1879 to explain the formation of the Santorini caldera and was mainly supported by the fact that the volume of older lithic rocks in the ejecta is much less than the missing structure. Scandone (1990) confirmed this hypothesis. By comparison between experimental results on formation of craters by conventional or nuclear devices and field observations concerning various caldera-forming eruptions (eruptive sequences, volume of ejecta, size of caldera, gravity anomalies...), he concluded that the energy required to form explosion crater with radii exceeding 500 m is never available during volcanic eruptions and, thus, that Krakatau caldera, as most calderas, could not have been generated by an explosion. As previously mentioned, the idea that the Krakatau vol-

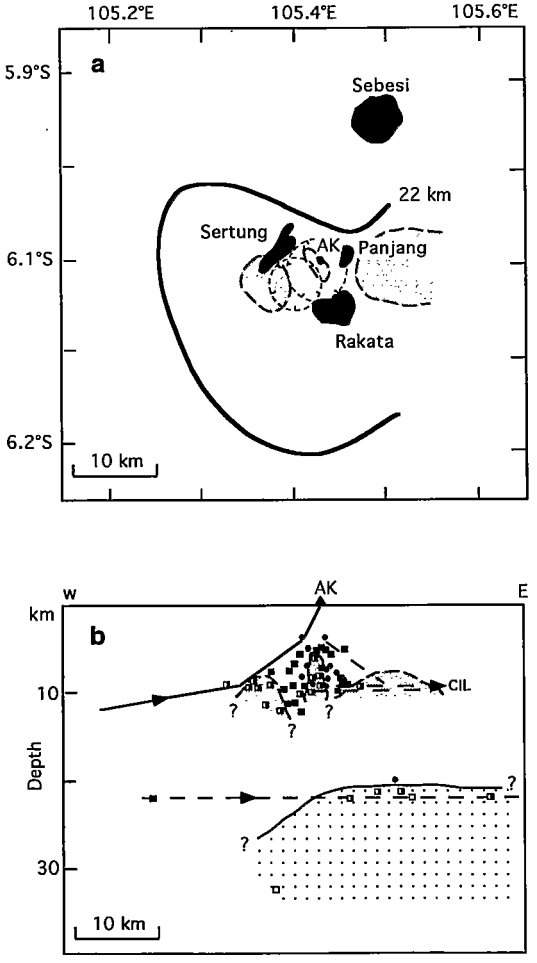

Fig. 3. Attenuation zones of S waves beneath the Krakatau volcanic complex (from Harjono et al., 1989). *AK*=Anak Krakatau (a) Surface projection: superficial (9 km depth) and deep (22 km depth) attenuation zones are indicated with shaded areas and with a solid line respectively. (b) West–east vertical section: attenuation zones appear in shaded areas.

cano would have been blown away by an explosion is dismissed in the current scenarios.

4.2. Microseismicity data

A temporary seismological network was installed in the Sunda Strait in 1984 in the framework of the French Indonesian Program. More than 600 local earthquakes were recorded (Harjono, 1988, Harjono et al., 1991). The analysis of S waves attenuation allowed some of us (Harjono et al., 1989) to detect beneath the Krakatau volcanic complex two anomalous zones (Fig. 3) which are assumed to correspond to two distinct magma reservoirs. The deeper one is located just beneath the Moho and presents a large horizontal extension. The upper one, located at a depth of about 9 km, has a smaller extension but is large enough to allow the differentiation of the volume of dacite of the 1883 eruption (G. Camus, pers. commun., 1988). It is divided into three parts that were interpreted as magma pockets. The depth found for this upper zone agrees well with the depth proposed for the magma chamber of Anak Krakatau according to petrological and geochemical results (Camus et al., 1987). Finally, as shown on Fig. 3, the present shape of this upper attenuation zone could be related to the internal structure of the volcano, controlled by the successive collapses of calderas, as proposed by Vincent et al. (1989).

5. Morphology of the Krakatau volcanic complex (bathymetry and topography data analysis)

5.1. Marine data acquisition

The marine data were collected during the Mentawai Cruise on board R/V *Baruna Jaya III* (Diament et al., 1991) (Fig. 4a). We used a narrow-beam echo-sounder for the bathymetry that gives more accurate estimations of steep slopes than classical equipment does. The navigation was achieved using GPS and TRANSIT satellite systems (the GPS system gave us a position every 13 seconds when a good constellation of satellites was available, that was about 22 hours a day). Due to the size of the vessel, data could be only collected in areas where the depth was large enough (Fig. 4b); for example, we could not record data just north of Anak due to the presence of shoals. Our data set completes well the bathymetric survey recently realized by Sigurdsson et al. (1991a,b) in shallow areas (less than 120 m).

5.2. Numerical model of altitude

The new bathymetric data were combined with those of two previous cruises (Corindon in 1983 and Krakatau in 1985) also conducted in the framework of the French–Indonesian program. In the areas where we have no data, especially in shallow areas, we used the bathymetric map published by the Volcanological Survey of Indonesia in 1982 on the basis of the data collected by Escher in 1919. Compilation of these data allows us to build a new bathymetric map extending up to 20 km around the volcanic complex. The data collected by Sigurdsson et al. (1991a) in shallow areas indicate only small differences with our compiled bathymetric map. Topography on the islands is given by both the altimetry data collected during our land survey and contour lines digitized from a topographic map of the volcanic complex (Volcanological Survey of Indonesia, 1982). A more detailed topographic map (1981, with corrections for the eruption of 1988) was used for Anak Krakatau. We used a portable GPS receiver to locate a few points on each island. The horizontal accuracy of the GPS equipment was checked on a geodetic bench mark, built up on Anak Krakatau during a GPS survey (M. Kasser, pers. commun., 1990), and is about 10 to 20 m. As a result of our accurate positioning in absolute geographical coordinates, we had to correct the previous published map by shifting and rotating some of the islands. This was possible because we located also some remarkable spots on the islands. After these corrections, the comparison between field altitude data (barometric and topographic levelling) and topographic maps shows only small discrepancies in the range of a few meters. A numerical model of altitude (bathymetry and topography) has thus been realized for a large area encompassing the Kraka-

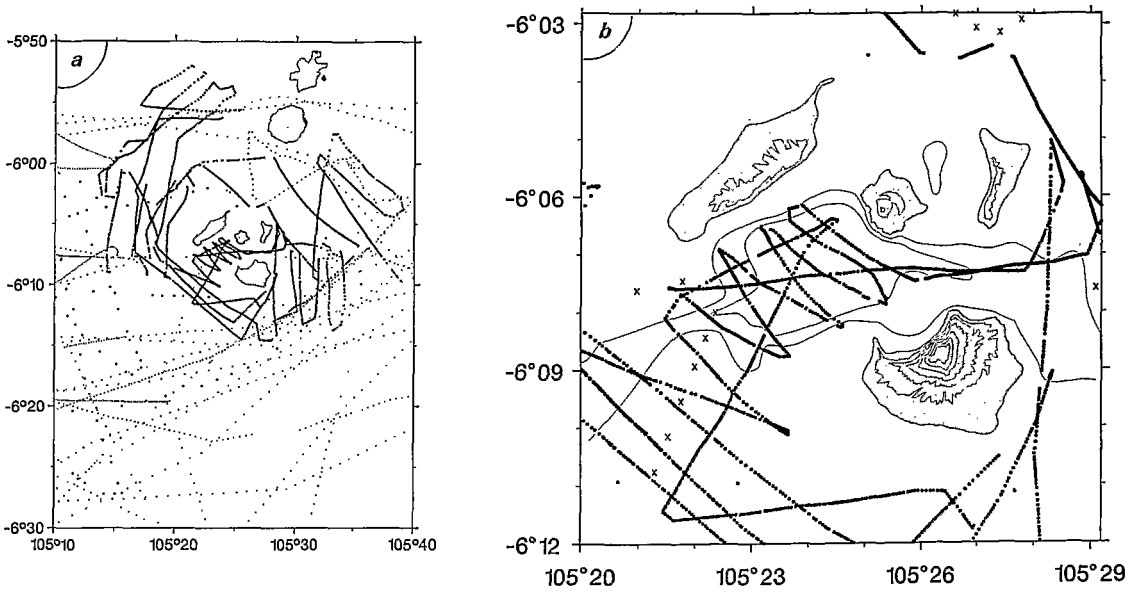

Fig. 4. Bathymetry data distribution. Large dots are data gathered during the Mentawai oceanographic cruise on board R/V *Baruna Jaya III* (1990). (a) Around the Krakatau area: small dots are data from previous cruises. (b) Detailed data distribution over the Krakatau complex. Crosses are data from Corindon oceanographic cruise (1983).

tau complex in order to compute the terrain corrections for the gravity data reduction. The central part of this model (6°12′S to 6°03′S and 105°20′E to 105°29′E) is shown on Fig. 5 on a 3-D representation. This area will be also used for the further gravity maps (anomaly and model). The 3-D view allows to identify the main effects of the 1883 eruption: the steep concave cliff of Rakata probably collapsed along the boundaries of the prehistoric caldera; the ignimbrite sub-marine deposits on the external sides of Sertung and Rakata islands (yellow shallow zones); the deep 1883 caldera (blue) resulting from the collapse of the roof of the magma chamber.

Note also the location of Anak Krakatau on the very edge of the 1883 caldera. A detailed view of Anak Krakatau seen from the southeast is shown in Fig. 6. The old crater rim and the new active cone are clearly shown on this representation. This emphasizes the migration of the volcanic activity in a southwestern direction and consequently toward the steep wall of the 1883 caldera. We discuss later the growth of Anak Krakatau on the edge of the 1883 caldera and its location on a probably unstable site.

5.3. Morphology of the caldera

General patterns

A detailed bathymetric map of the caldera contoured every 20 meters is shown on Fig. 7. The bathymetric depression is elongated in shape with two main directions: southwest–northeast and west–east to the west and east of Anak Krakatau, respectively. The deepest part (A on Fig. 7) is located southwest of Anak Krakatau and has a rectangular shape with a flat bottom (240 m below sea level) and steep linear walls. Leading out this flat deep area towards southwest and east are elongated grabens with floors deeper than 100 m. A careful examination of our bathymetric records to the west of the caldera shows that the narrow graben cutting the western wall of the

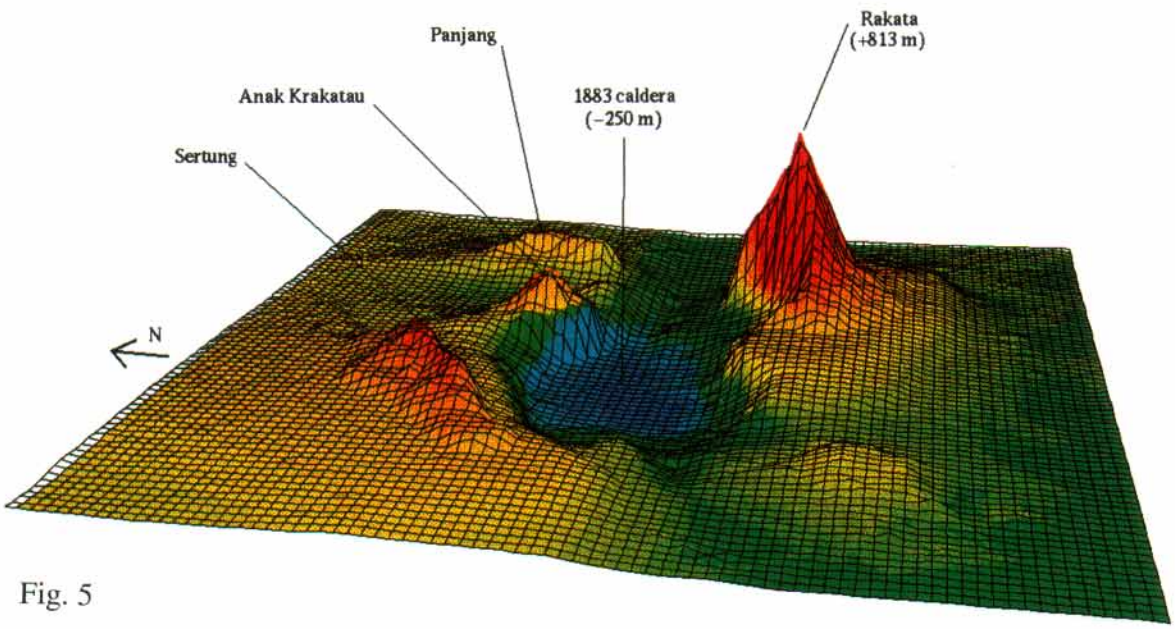

Fig. 5

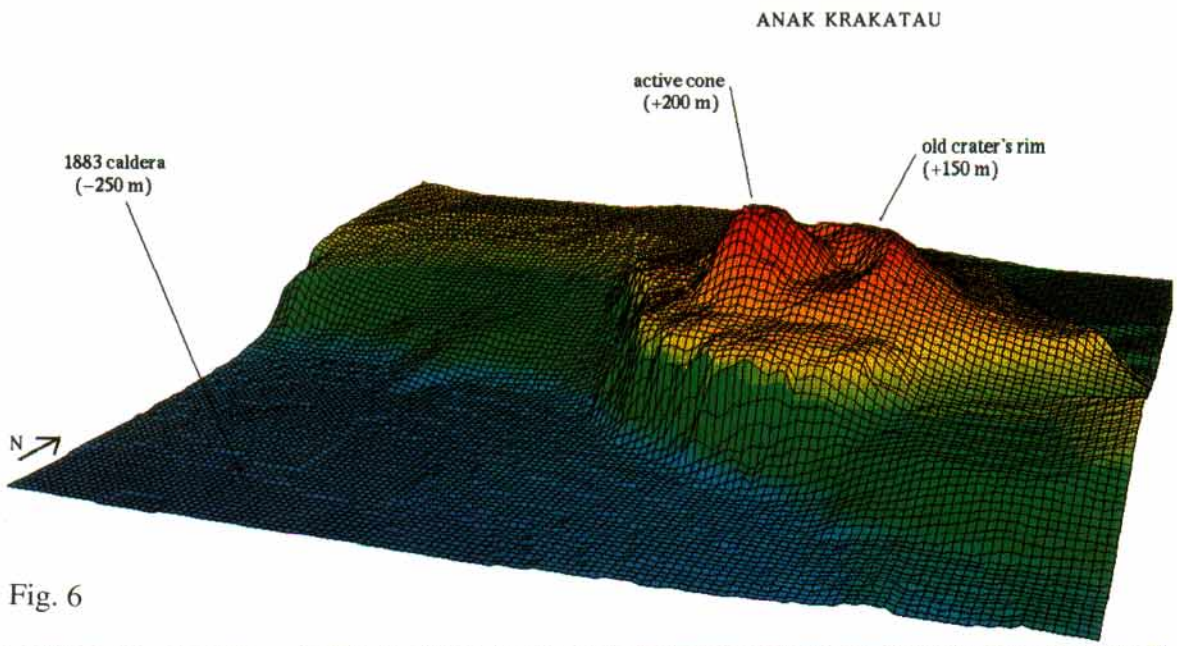

Fig. 6

Fig. 5. Three-dimensional Numerical Model of Altitude (NMA) of the Krakatau volcanic complex (view from the west). The NMA is obtained from interpolation of bathymetry data gathered during oceanographic cruises and digitized data from existing topographic and bathymetric maps within a 17×17 km area. A logarithmic color scale is used to represent the bathymetric and topographic variations between −250 m (bottom of 1883 caldera, in blue) and +813 m (summit of Rakata island, in red); the sea surface is approximately between the orange and yellow color levels.

Fig. 6. Three-dimensional Numeric Model of Altitude (NMA) of Anak Krakatau (see legend of Fig. 5 for NMA construction. This view is from the South East. The logarithmic color scale represents the bathymetric and topographic variations between −250 m (bottom of 1883 caldera, in blue) and +200 m (summit of the active cone, in red).

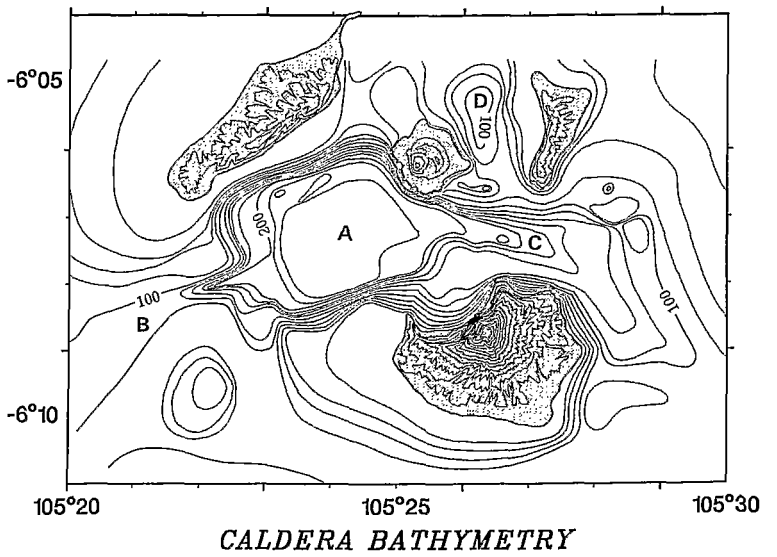

Fig. 7. Detailed bathymetric map of the 1883 caldera drawn from data gathered during the MENTAWAI cruise (1990) and digitized data from existing bathymetric maps. Isolines are drawn every 20 m and solid lines represent curves −100 and −200 m.

caldera is prolonged by a linear depression 20 m deep (B on Fig. 7). We previously suggested (Harjono, 1988; Diament et al., 1990) that Krakatau lies just at the intersection of the N20° volcanic line with a transverse feature, oriented N50°, that links Krakatau to the Sunda Strait graben. This N50° feature was interpreted as a fault on the base of its seismological and gravimetric signatures. The bathymetric depression to the west of the caldera corresponds probably to the termination of that fault. Since strong underwater currents are reported in the vicinity of the Krakatau complex, we believe that the formation of this narrow graben is a consequence of a submarine erosion along the N50° fault.

The north and south walls of the deepest part are oriented N70° with slopes of about 20°. The direction of these walls is roughly parallel to the one of the above-mentioned fault. The east and west walls are oriented N150°, and the slope on the western one is smaller of about 7°. The N150° azimuth corresponds to the direction on which the former vents of the pre-1883 Krakatau island, Danan and Perbuatan were lying (see Fig. 2). In addition, Stehn (1929) reported that in January 1928, when Anak Krakatau emerged above sea level, "*the eruptions were not proceeding from a single point but that rather there were six crater openings arranged in a line about* 500 *meters in the NNW–SSE*" (i.e. N150°). We propose that the N150° azimuth, along which craters are aligned, corresponds to a structural direction that has partly controlled the caldera formation.

Therefore, analysis of our new data confirms that the shape of the caldera is associated to linear directions corresponding to tectonic features. Thus, we agree with Williams (1941) who assumed that the collapse of the caldera has been controlled by pre-existing features. In 1968, Oide already noted that the Japanese Krakatau-type calderas are mostly rectangular in outline and that their straight boundaries have received few attention.

Although, our data do not extend very close to the Rakata steep cliff (see Fig. 4b) we can precise the shape of the contour lines north of Rakata. This shape may be related to a flow of material coming from the cliff that could correspond to slumping or rolling down materials. This could be in agreement with Francis and Self assumptions (1983) which supposed that the cone of

Rakata was apparently left perched on the southern rim of the caldera after the caldera collapsed, then slumped into the sea. Moreover, two weeks after the paroxysm and 9 months later, rock-fall dust clouds, that were initially mistaken for volcanic activity, have been observed. Such clouds were also seen in 1896 and 1897 (Simkin and Fiske, 1983). Rock-falls along Rakata cliff have been also reported by Cool in 1908 (in Simkin and Fiske, 1983). Nevertheless, a detailed survey of the submarine foot of the Rakata cliff is necessary to precise this point.

Changes in the caldera since 1883

The bathymetry of the inner part of the Krakatau complex after the 1883 eruption has been known at different times. Soundings were started shortly after the 1883 eruption (Verbeek, 1885) by the survey ship *Hydrograaf*. Then, numerous soundings collected in 1919 (bathymetric map published by Escher in 1919) and a few supplementary ones in 1922–1923 (Escher, 1928, in Stehn, 1929) have shown that changes have occurred: the caldera had become deeper. Examination of the submarine profiles has convinced Neumann van Padang (1933) that this deepening of the caldera represented a vertical sagging. This strongly suggests a compaction of the materials filling up the caldera.

Comparison of our map with the one of Escher (in Stehn, 1929) reveals some differences. The bottom of the caldera is more flat: the two small 25-m depressions flanking a N–S central ridge, that were shown on Escher's map, are no more present. The walls of the caldera appear now to be steeper and more rectilinear. Moreover, the bottom of the caldera is now less deep: on average, 240 m b.s.l. instead of 250 m b.s.l. and the maximum depth is 255 m b.s.l. instead of 279 m b.s.l. Both the erosion of ignimbrite deposits and the products from Anak might be advocated in order to explain this apparent infill of the caldera.

Sudrajat (1982), on the base of a few soundings obtained in 1940, already noticed that the deepest part of the caldera had become shallower from 279 m b.s.l. to approximately 250 m b.s.l.. He suggested that this was due to the sedimentation of the volcanic products from Anak Krakatau and he has estimated the rate of sedimentation to be about 1 to 3.5 m per year between 1919 and 1940. According to the fact that the frequency of eruptions of Anak seems to be quite constant, Sudrajat also proposed that this rate of sedimentation remained identical between 1940 and 1982. Our data show that the depth of the bottom of the caldera did not really changed since 1940. That can be explained by both a slowing down of the erosion of ignimbrite deposits and by the fact that the activity of Anak became exclusively aerial since 1960.

5.4. Growth of Anak Krakatau

Anak Krakatau is born about midway between the former craters of Danan and Perbuatan, where the main vent for the 1883 eruption is supposed to have laid (following the consensus opinion), immediately off the steep NE wall of the basin formed by the collapse of the 1883 caldera. According to Stehn (1929), the position of the eruption point corresponded nearly to a former depth point of 188 meters (soundings of 1919). Rapid soundings at the end of January 1928 have shown that the western slope of the volcano was considerably steeper than the eastern. This was interpreted by Stehn (1929) as a consequence of its position right off the steep wall of the basin and also of the strong current that was generally running southwest to northeast. Figure 8 displays the temporal evolution of a SW–NE morphological profile from 1919 to the present day. We also show the location of our data closest to Anak. Clearly, Anak Krakatau was built on the flank of the caldera (slope estimated of about 18° in 1919). The build up of new cones on the flank of collapse calderas was also observed in Campi Flegrei (Scandone et al., 1991) and for Santorini (Heiken and McCoy, 1984). In 1928, the southwestern slope of Anak was steeper as 29°. Nowadays, this slope seems to be still important and shows that the successive eruptions did not resulted in a gentle filling of the caldera. Indeed, our data show that at a distance of 900 m from the shore of Anak, the depth is 245 m b.s.l. and that there is no indication of a gentle rise. Therefore the actual slope of the

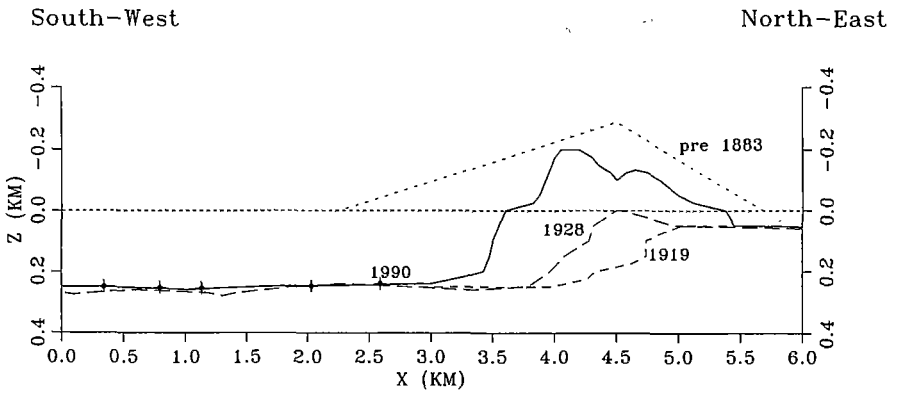

Fig. 8. Morphological evolution with time of Anak Krakatau along a SW–NE line. Dashed lines below the sea level are the bathymetric profiles in 1919 and 1928. Solid line is the actual morphology of Anak Krakatau along which the nearest bathymetry data gathered during the MENTAWAI cruise 1990 (dots) have been reported. Dashed line above the sea level shows the mean topography of the Krakatau island before the 1883 eruption.

western submarine flank of Anak Krakatau is at least 15°. Note that on Fig. 7, we used the bathymetric contour lines of the map published by the Volcanological Survey of Indonesia on which the southwestern flank of Anak is not really constrained by data. Nevertheless, our data obtained on board the *Baruna Jaya III* show that its southwestern flank is steep and since Anak is growing towards the southwest, one cannot exclude landslides along this flank. Several few meters tsunamis occurred probably there in 1981 (Camus et al., 1987; Sigurdsson et al., 1991b). Obviously, a more detailed survey of the slope should be realized in the future.

6. Inner structure (gravity data analysis)

6.1. Land data acquisition

In 1990, we realized 148 new gravity measurements on the Krakatau volcanic complex. The gravity stations are located on a few profiles through Panjang, Sertung and Rakata islands and on a dense network on Anak Krakatau (Fig. 9). Gravity readings were made with two Lacoste and Romberg gravity meters (G and D model). A gravity base was installed on Sertung and tied to the IGSN71 base of Waymuli, located on the SouthWest coast of Sumatra. We used the algorithm of Longman (1959) for the earth tide correction. The accuracy of the gravity measurements is about 0.05 mGal.

On each island, the gravity stations were tied with optical devices (theodolite and EDM) from the network of approximately 30 stations located with GPS. The absolute horizontal positioning of all gravity stations is within 10 to 20 m.

A precise levelling of the gravity stations has been done with optical devices. The accuracy is within a few centimeters. For some stations along the shore of the islands and on Anak, the altitude data were determined by barometric levelling. The accuracy of the barometric levelling is better than 2 m, precision that is enough for the gravity modelling of the deep structure of the volcano.

The irregular distribution of the gravity stations shown on Fig. 9b relates the field conditions. Except Anak Krakatau, the vegetation is extremely dense on the islands due to the tropical climate. Moreover, the topography is very rough, cut with numerous incised valleys consequence of the strong erosion over the pumice deposits. Verbeek (1885) reported in October 1883, two months after the eruption, that steep-sided gullies 40 m deep had been already cut into

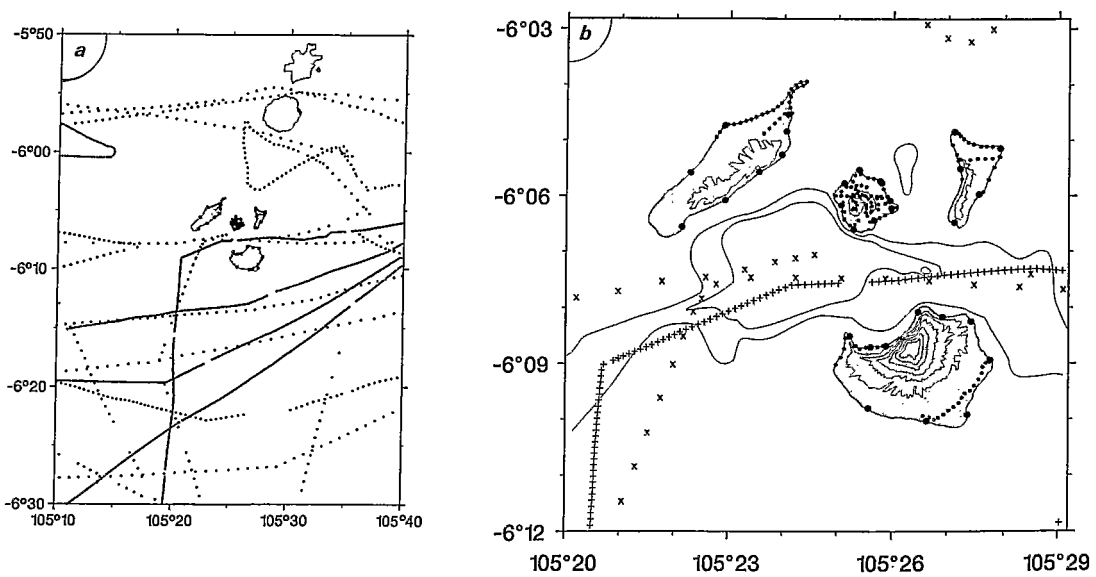

Fig. 9. Gravity data distribution. Data come from land surveys (this survey; Yokoyama, 1969, 1982) and oceanographic cruises (Corindon'83 and Krakatau'85). (a) Around the Krakatau area. (b) Detailed gravity data distribution over the Krakatau volcanic complex. Land data: small dots are data from this survey and large dots are data from Yokoyama and Hadikusumo, 1969; Yokoyama, 1982. Marine data: symbols '+' and 'x' consist in data from Krakatau and Corindon cruises, respectively.

the deposits. As the islands are uninhabited, no paths exist inside the islands and the optical sightings in the forest was limited to 25 m, slowing down the surveyors progression to 500 m per day. On another hand, landing on the shores appeared to be quite difficult in some places, and even impossible (along the western and southern coast of Sertung for example), due to the presence of crumbling sea cliffs.

6.2. Complete Bouguer anomaly

Data compilation

In order to compute the Bouguer anomaly map of the Krakatau complex, we used all data available in this area (Fig. 9). We added the land data previously published by Yokoyama and Hadikusumo (1969) and Yokoyama (1987) and the sea surface data recorded during Corindon and Krakatau cruises (Diament et al., 1990). All data were tied to the IGSN71 system. The cross-over analysis of the sea surface gravity data shows a good agreement between the two cruises since the discrepancies of free air anomaly at crossing points are less than 2.5 mGal, i.e. the accuracy of marine gravity data. Comparison of our land data with the nearby data of Yokoyama show differences of less than 1 mGal on free air values. A set of 180 land data and 337 sea surface data was used to compute the Bouguer anomaly map.

Data reduction

The observed gravity value g is reduced to Bouguer anomaly g_{AB} by:

$$g_{AB} = g - \gamma + \beta h - 2\pi G \rho h + T(\rho)$$

(on land data) (1)

$$g_{AB} = g - \gamma + 2\pi G(\rho - \rho_w)d + T(\rho)$$

(sea surface data) (2)

where γ is the normal gravity value in IGSN71 system, β is the vertical gradient of the normal gravity (estimated at 0.3086 mGal/m), G the

Newton gravitational constant, ρ the reference density, ρ_w the sea water density is 1.03 g/cm^3 and $T(\rho)$ is the terrain correction; h is the station elevation for on-land data and d the depth of the sea-floor below a sea-surface gravity measurement. According to the definition of Bouguer anomaly, the Bouguer anomaly refers to the topographic surface for on-land data (Patella, 1988) and to the sea-level for marine data.

In order to take into account the large topographic and bathymetric variations of the studied area, we computed terrain corrections at every gravity data location. For that purpose we used the numerical model of altitude (NMA) previously described, extending up to 20 km around the volcanic complex. Using bathymetric and topographic contour lines, we represented the NMA as a pile of prisms. Horizontal geometry of each prism is directly given by the shape of the contour lines and their thickness is equal to the altitude difference between two contour lines. This thickness depends upon the accuracy of the data used for the NMA and is of 12.5 m for Anak topography, 25 m for bathymetry and 50 m for topography of the outer islands of the complex. The terrain correction is then computed at each data point by summing the gravity effects of horizontal faces of the prisms. The algorithm used to compute the gravity effect of a plane facet is given by Chapman (1979). We will use the same computation method for the 3-D gravity modelling described later on.

The total terrain correction at a data point is $T(\rho)=\rho T_{\text{land}}+(\rho_w-\rho)\,T_{\text{sea-bottom}}$ where T_{land} and $T_{\text{sea-bottom}}$ are terrain corrections, for unit density, due to the emerged and immerged part of the NMA respectively. Maximum values for the terrain correction are 9 mGal at the top of Anak and 8 mGal for points located close to the Rakata cliff. The use of a step-like topographic model instead of a regular slope model introduces an error smaller than 1 mGal. This error depends on the thickness of the prisms, for example on Anak the error is less than 0.4 mGal (Dahrin, 1993).

For a given reference density, the final accuracy of the Bouguer anomaly is estimated at ± 1 mGal for land data and ± 2.5 mGal for sea surface data.

Density determination

A critical point in the computation of Bouguer anomaly is the choice of the density for the slab and terrain corrections. As no rock density measurements are available for the whole Krakatau volcanic complex (islands and submarine deposits), we applied the Nettleton (1976) and the Parasnis methods (1962) on the gravity data. These methods have only good application within areas characterized by homogeneous density and where there is no correlation between the topography and the Bouguer anomaly (Williams and Finn, 1985). They have to be used carefully in volcanic areas where the reliefs are made of heterogeneous structures. In the Nettleton method (1976), the density is adjusted to minimize the correlation between the complete Bouguer anomaly and the topography. We have computed Bouguer anomaly maps for various densities ranging from 1.9 to 2.7 g/cm^3 with a 0.1-g/cm^3 step. The resulting maps show that no density minimizes the correlation for the whole volcanic complex. In fact, a poor correlation is obtained on the outer islands for high density values while the correlation is minimized over Anak for lower densities. This information will be later used and discussed in the modelling of the Bouguer anomaly.

Parasnis (1962) proposed an analytical approach to estimate the average superficial density. From Eq. (1) one can write:

$$Y=2\pi G\rho_B X+g_{AB} \tag{3}$$

with $Y=g-\gamma+\beta h+T(\rho_T)$ and $X=h$.

Assuming g_{AB} to be a random error of mean value constant in the study area, the slope of the best-fit straight line for the plot of Y versus X will give ρ_B for a given value of ρ_T. The retained density ρ_B is such that it equals the assumed ρ_T. Of course this method is only valid in areas with small variations of Bouguer anomaly compared to the variations of the slab corrections, that is in areas with important altitude changes and constant geology. Therefore, the only zone where this method can be applied is the southwestern part

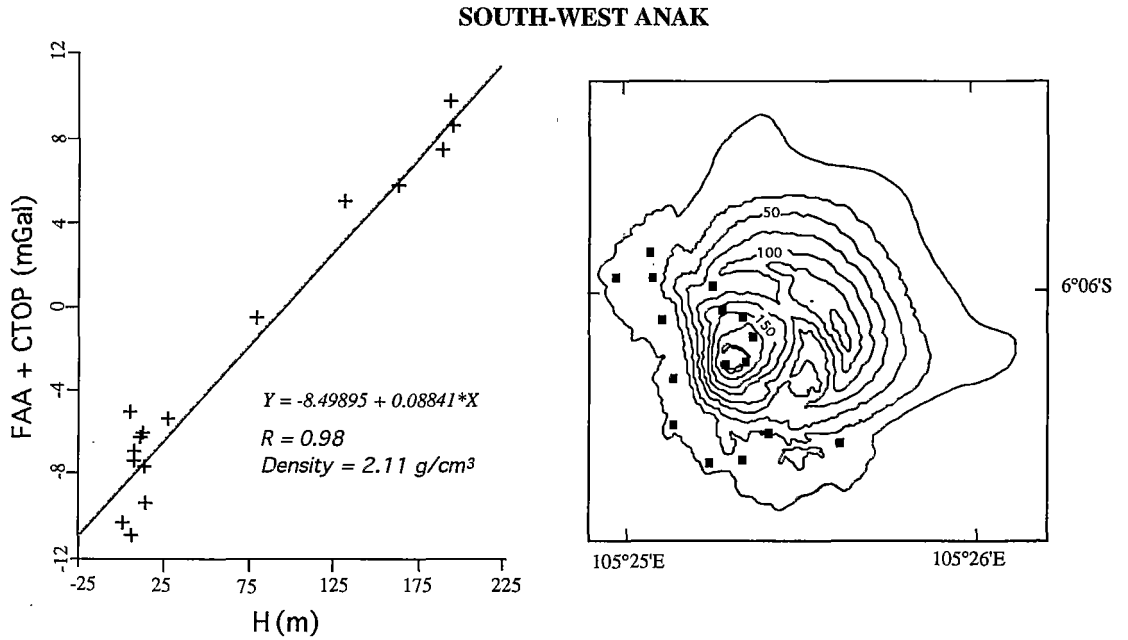

Fig. 10. Density determination on Anak Krakatau by means of Parasnis method. The method is applied on data from southwest of Anak Krakatau (black squares on right side). Over this geologically homogenous area, the topographic variations are large while the Bouguer anomaly is nearly constant. On left side: free-air anomalies plus terrain correction plotted versus height of the station. Varying the density for terrain correction by step of 0.1 g/cm^3, the best fit is obtained for 2.1 g/cm^3 (see text). This value consisting in the mean density of recent volcanic products, is used as density reference for gravity reductions and gravity modelling.

of Anak where many lava flows were emplaced since 1970. The resulting density value is of 2.1 g/cm^3 (Fig. 10). This low value characterizes recent products from Anak and is comparable to the surface density found on other volcanoes (Williams and Finn, 1985). Moreover, it is interesting to note that Verbeek (1885) gave a value of 2.2 g/cm^3 for the density of the fine products of the 1883 eruption, these products covering the sea-bottom and the outer islands of the complex. Furthermore, a density close to 2.1 g/cm^3 for the upper sedimentary layer around the Krakatau complex has been deduced from velocities obtained by a refraction study west of Krakatau (Larue, 1983) and from drilling data in the eastern part of the Sunda Strait (Noujaim, 1976). Therefore, we decided to use a reference value of 2.1 g/cm^3 for the reduction of gravity data.

Bouguer anomaly map

Figure 11a shows the Bouguer anomaly map for the density of 2.1 g/cm^3. According to the data distribution, we preferred to draw the contour map by hand rather than to use any interpolation algorithm that could introduce spurious effect. This map reveals a ring of high gravity over the external islands of the complex. The average amplitude of this anomaly is +77 mGal with local maxima on Rakata, Sertung (+82 mGal), and Panjang (+80 mGal) islands. To the southwest, the amplitude of the positive anomaly decreases down to +75 mGal. A sub-circular low anomaly of +54 mGal lies in the middle of the high ring. Note that Anak Krakatau is located on the steep linear gradient between the minimum and maximum anomalies. This N150° gradient underlines the already mentioned direction passing through the ancient

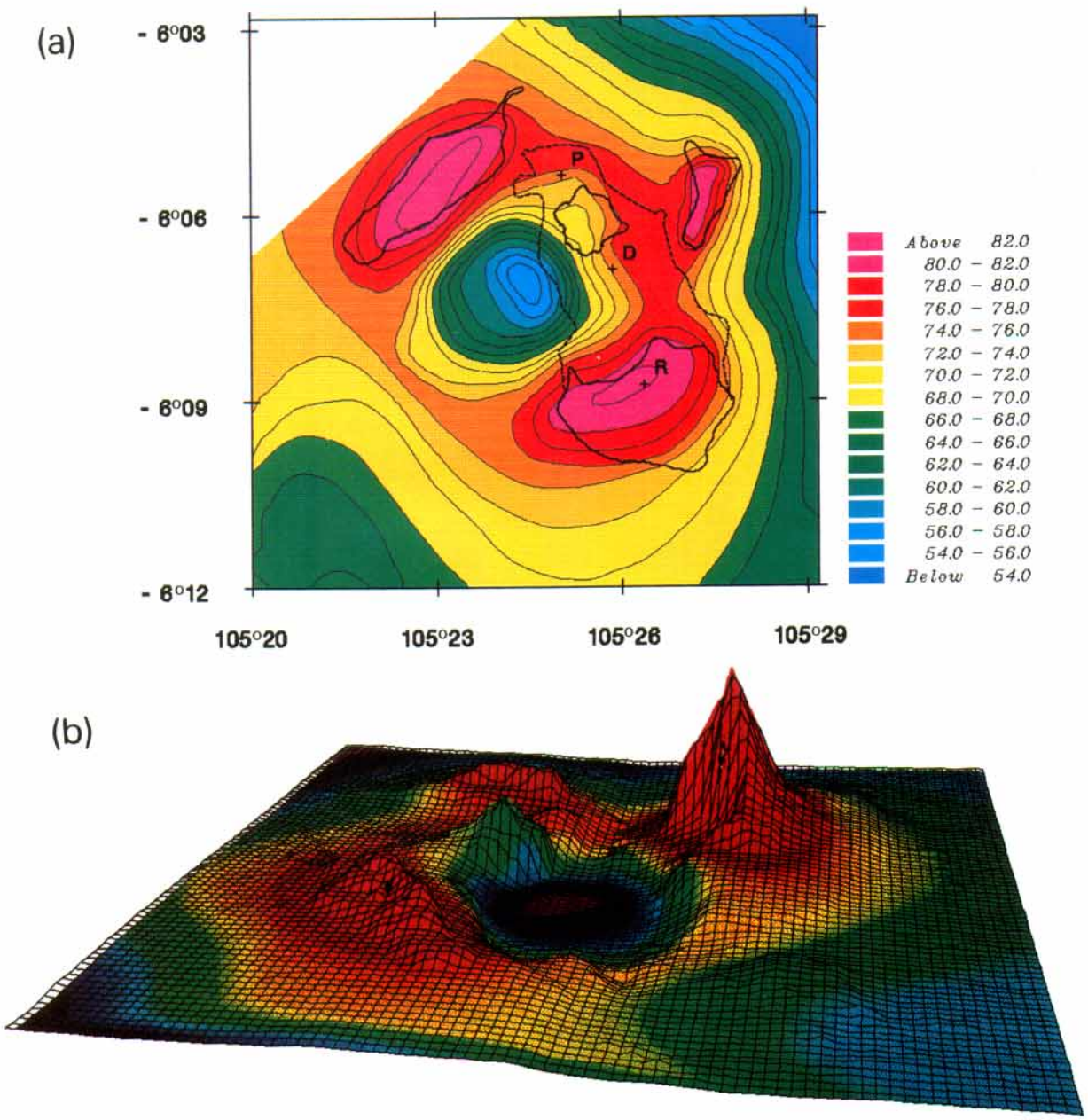

Fig. 11. (a) Bouguer anomaly map of Krakatau volcanic complex (mGal). The map is computed in IGSN71 reference system for a 2.1 g/cm^3 density reference. The coastline of the Krakatau island before the 1883 eruption appears in dashed line; *R*, *D* and *P* denotes its old active centers Rakata, Danan and Perbuatan respectively. (b) Bouguer anomaly map of Krakatau volcanic complex superimposed over the 3D Numeric Model of Altitude. The color scale shows the variation of the Bouguer anomaly from +54 mGal (purple) to +82 mGal (red). This graphic representation emphasizes the relations between the Bouguer anomaly and the morphology of the complex. No correlation remains between gravity anomaly and topography on Anak Krakatau. In the same way, there is no correlation along the ring between Bouguer anomaly and the bathymetry of the sea-floor. This indicates that 2.1 g/cm^3 is a good value for the average density of Anak and also for volcanic products covering the sea-bottom and the outer islands. A remarkable feature is the correlation between gradients of the low gravity anomaly and the morphology of the 1883 caldera. This correlation indicates a probable superficial origin related with the caldera development.

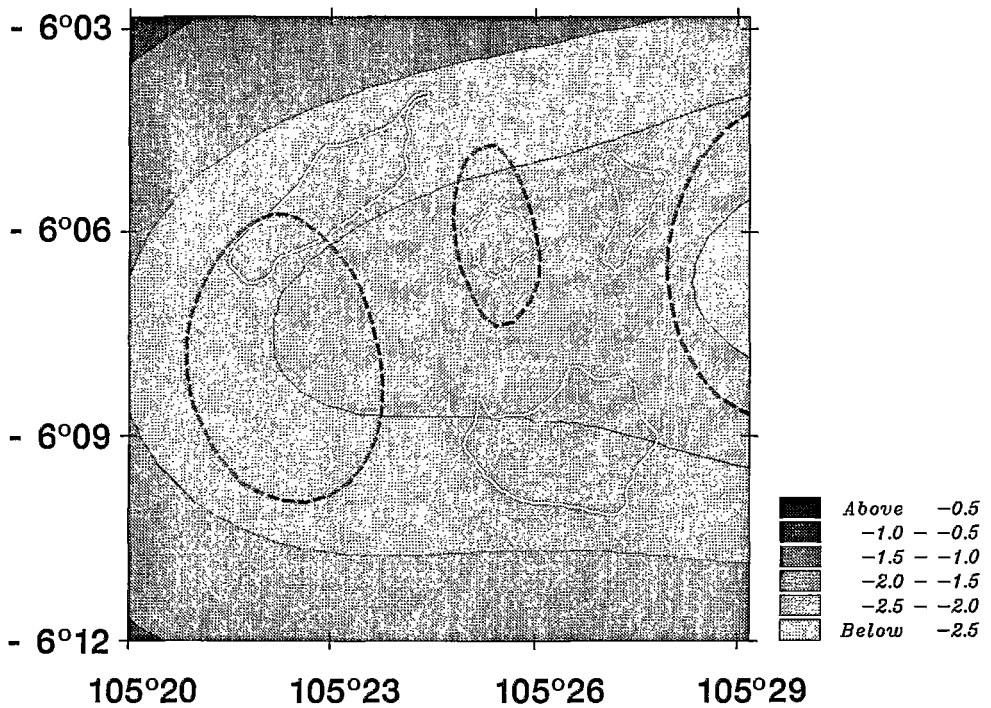

Fig. 12. Gravity effect of superficial magma chambers deduced from the seismological study of Harjono et al. (1989). The effect is computed in mGal using a mean density of -0.2 g/cm^3 and the 3-D geometry shown in Fig. 3. Horizontal extension of the three superficial magma chambers at 9 km depth appears in dashed lines.

craters of Danan and Perbuatan and the present active one. Outside the positive ring, the Bouguer anomaly is roughly of +65 mGal, consistent with the regional trend deduced from the free-air gravity map of the Sunda Strait (Diament et al., 1990).

No correlation remains between gravity anomaly and topography on Anak Krakatau (Fig. 11b). This confirms that 2.1 g/cm^3 is a good value for the average density of Anak. In the same way, there is no correlation along the ring between Bouguer anomaly and the bathymetry of the sea-floor. This indicates that 2.1 g/cm^3 is also a good value for volcanic products covering the sea-bottom and the outer islands. Therefore, the Bouguer anomaly primarily reflects density heterogeneities beneath the sea-floor and cannot be related to a deficient terrain correction. Furthermore, Anak Krakatau is underlined by a much smaller anomaly than the other islands of the complex indicating higher density values beneath the outer islands. Finally, there is a clear spatial relationship between the minimum of the anomaly and the 1883 caldera morphology: the highest gravity gradients closely follow the steep flanks of the caldera. Such correlation is an indication that the source of this relative negative anomaly is mainly superficial.

6.4. Gravity interpretation (3-D gravity model)

Gravity anomaly over calderas

The Bouguer anomaly map of the Krakatau presents similar characteristics to those obtained on other volcanic complex such as Santorini volcano (Budetta et al., 1984) or Campi Flegrei (Barberi et al., 1991; Fedi et al., 1991). All these maps exhibit a negative anomaly over a caldera surrounded by a ring of positive anomalies. According to Rymer and Brown (1986), negative anomalies are mostly observed on volcanic complexes with a long history of explosive eruptions

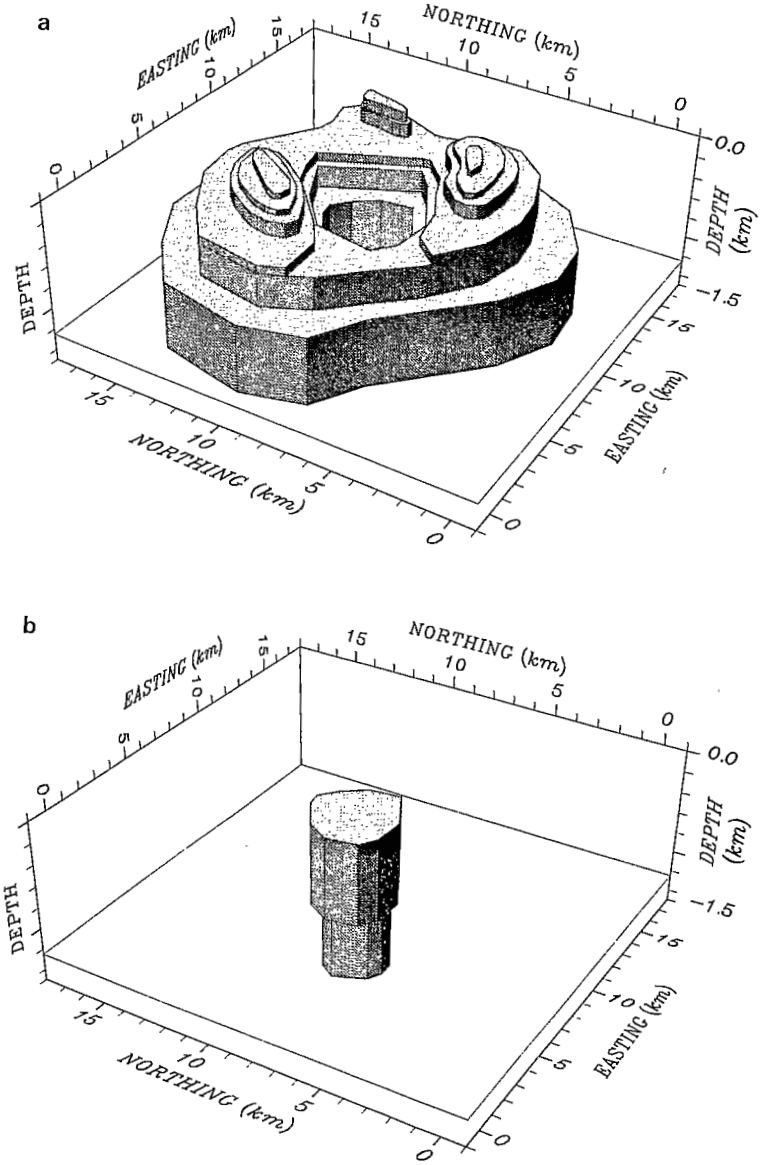

Fig. 13. 3-D geometry of our best-fit density model. (a) High-density body (density contrast of $+0.5$ g/cm^3) interpreted as the volcanic substratum of the proto-Krakatau. (b) Low-density body (density contrast of -0.2 g/cm^3) interpreted as a mixing of juvenile products of the 1883 eruption and lithic remnants of the destructed volcano filling up the 1883 caldera.

associated with caldera formation and emission of highly silicic pyroclastic materials. Such volcanoes are found on continental crust in a subduction or rift environment (e.g., Long Valley, Yellowstone, Japanese and Indonesian volcanoes...). In each case, there is a close correlation between anomaly wavelength and caldera diameter indicating a strong genetic relationship. Low-density caldera infill, often silicic pyroclastic material, is probably responsible for the observed negative anomaly while denser volcanic rocks forming the volcano substratum are fre-

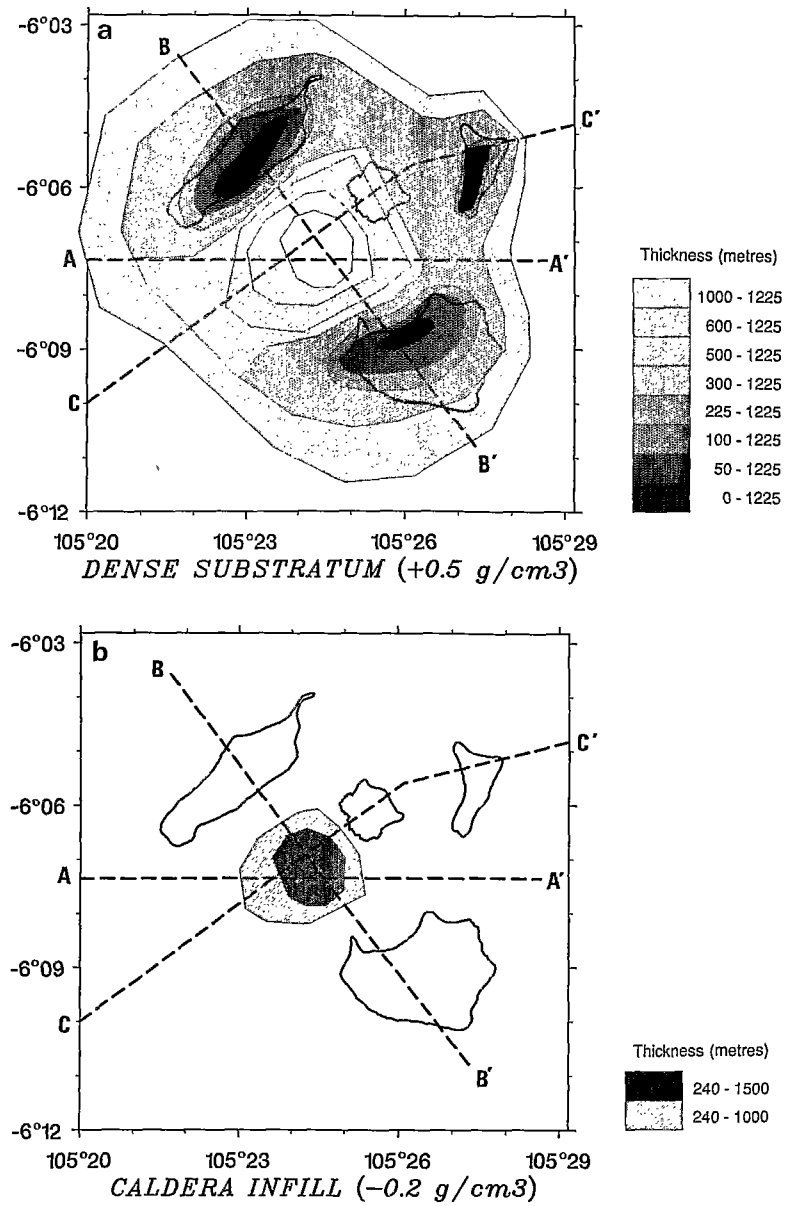

Fig. 14. Horizontal geometry of the 3-D density model shown in Fig. 13. The grey color scale indicates the thickness of the density body below the sea surface. *AA'*, *BB'* and *CC'* gives the location of the cross-sections shown on Fig. 15. (a) High-density body: dense substratum. (b) Low-density body: caldera infill.

Fig. 15. Vertical sections of the 3-D density model along lines AA' (a), BB' (b) and CC' (c) (see location on Fig. 14). (I) Observed and computed gravity anomalies in mGal. The observed values at gravity stations are shown with dots on the observed anomaly (dashed line). Error bars are ±1mGal and ±2.5 mGal for land and marine data, respectively. Light solid lines show the gravity effects of low- and high-density bodies. The total computed anomaly (heavy solid line) fits the observed anomaly within the precision of the data. A constant regional value of +62 mGal has been added to all computed gravity effects. (II) Complete density model extending down to a depth of 8 km. The reference density model (on the right) is based on the results of a refraction data analysis (Larue et al., 1983). All values of density are in g/cm^3. (III) Detailed superficial part of the density model from 0 to 2 km depth.

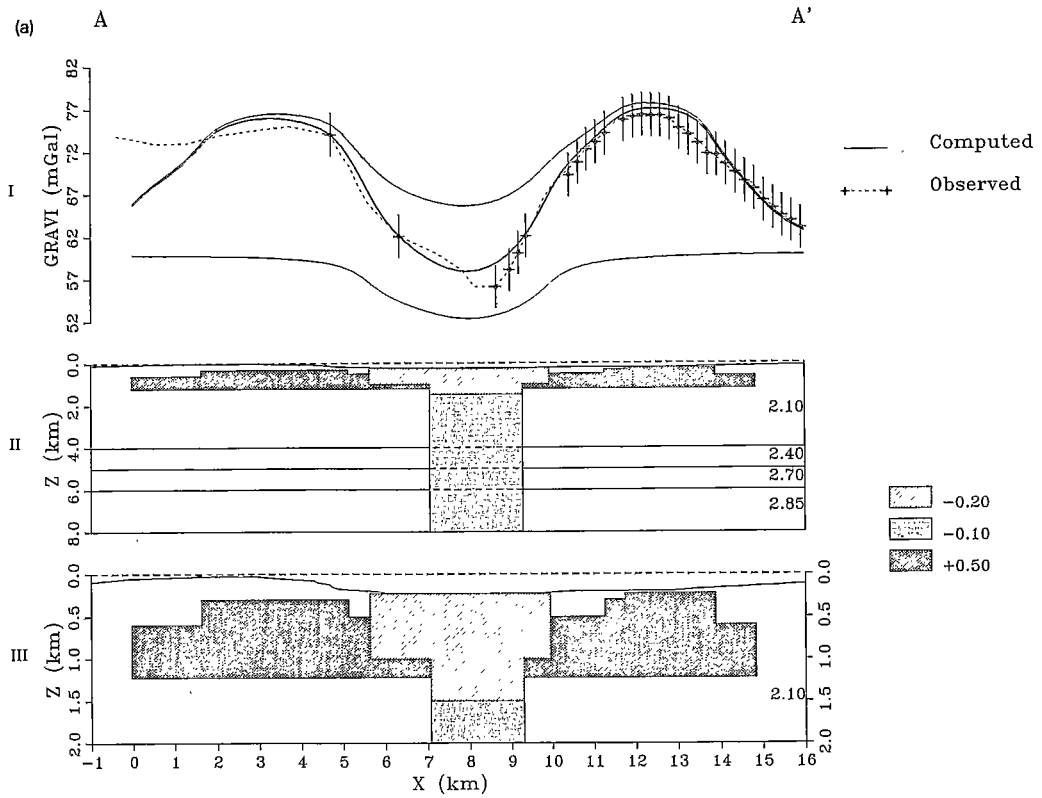
(a)
A
A'
I
GRAVI (mGal)
82
77
72
67
62
57
52
Computed
Observed
II
Z (km)
0.0
2.0
4.0
6.0
8.0
2.10
2.40
2.70
2.85
−0.20
−0.10
+0.50
III
Z (km)
0.0
0.5
1.0
1.5
2.0
2.10
−1
0
1
2
3
4
5
6
7
8
9
10
11
12
13
14
15
16
X (km)

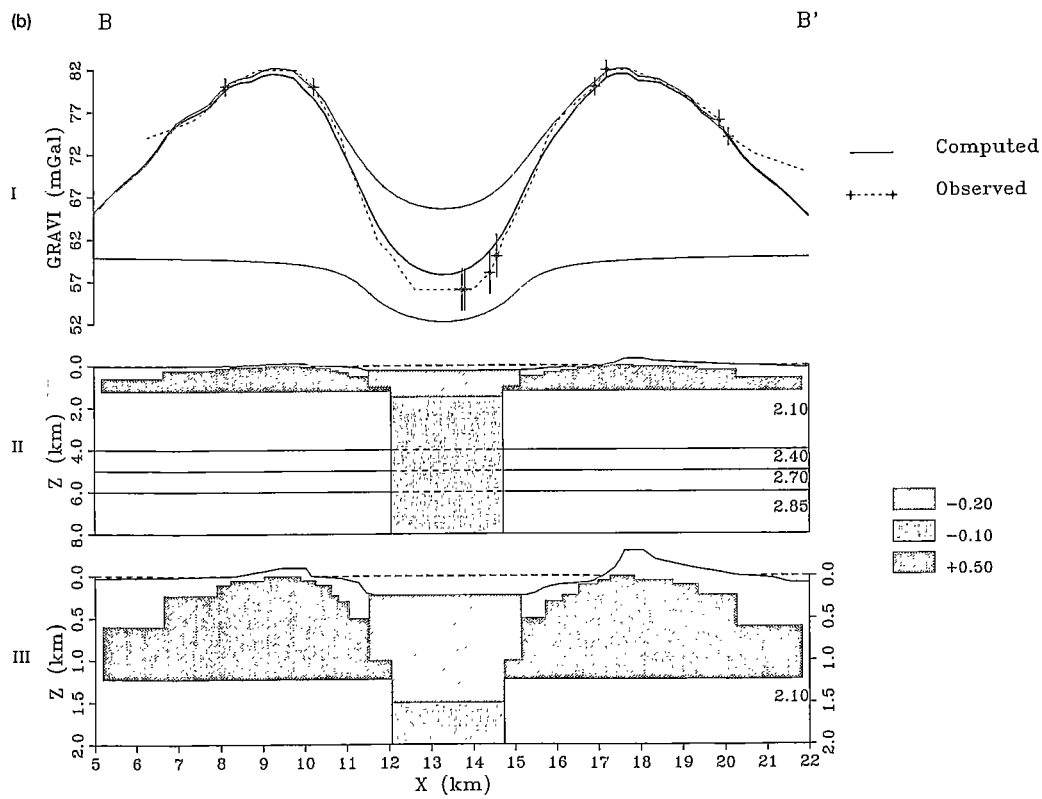
(b)
B
B'
I
GRAVI (mGal)
82
77
72
67
62
57
52
Computed
Observed
II
Z (km)
0.0
2.0
4.0
6.0
8.0
2.10
2.40
2.70
2.85
−0.20
−0.10
+0.50
III
Z (km)
0.0
0.5
1.0
1.5
2.0
2.10
5
6
7
8
9
10
11
12
13
14
15
16
17
18
19
20
21
22
X (km)

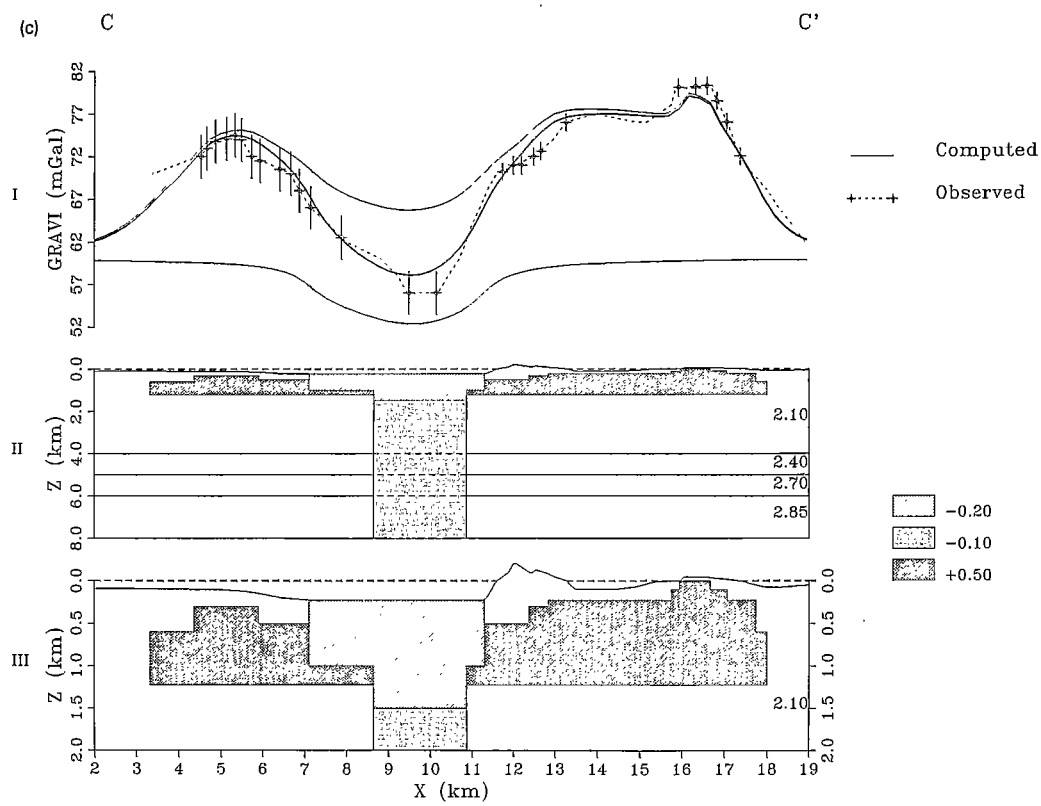

Fig. 15. (continued).

quently invoked as source of the positive ring. In the case of an active volcano, a low-density magma chamber within the uppermost few kilometers of the crust may also contribute to the gravity low (Kane et al., 1976; Yokoyama, 1981; Rymer and Brown, 1986; Scandone, 1990).

The gravity effect of magma chambers

In order to interpret the observed gravity anomaly over the Krakatau volcanic complex, we first determine the contribution to the gravity low of the magma bodies imaged by Harjono et al. (1989) from anomalous S waves. Although some uncertainty exists for the density contrast of a magma body, it is generally assumed to be negative and less than 0.5 g/cm^3 (Isherwood, 1976; Iyer, 1984; Blake and Ivey, 1986; Rymer and Brown, 1986; Brown et al., 1987; Scandone, 1990). Figure 12 displays the gravity effect of the superficial magma chambers, computed using a density contrast of -0.2 g/cm^3 and the 3-D geometry deduced from the seismological study and shown on Fig. 3. This effect is elongated in the east–west direction and is of small amplitude and large wavelength and thus contributes slightly to the observed anomaly. Since the amplitude variation (1.5 mGal) within the area is of the order of the accuracy of our Bouguer anomaly, we will not further consider this contribution in our modelling. Note that the deep attenuation zone revealed by the tomographic study and located at the Moho is too large and too deep to produce any local gravity effect and thus will neither be taken into account. Introducing a denser crystallised roof for a more realistic model of a magma chamber, as proposed by Scandone (1990), will also decrease the amplitude of the gravity effect. Therefore, the observed gravity anomaly over the Krakatau area is mostly controlled by the subsurface inner structure of the volcanic complex.

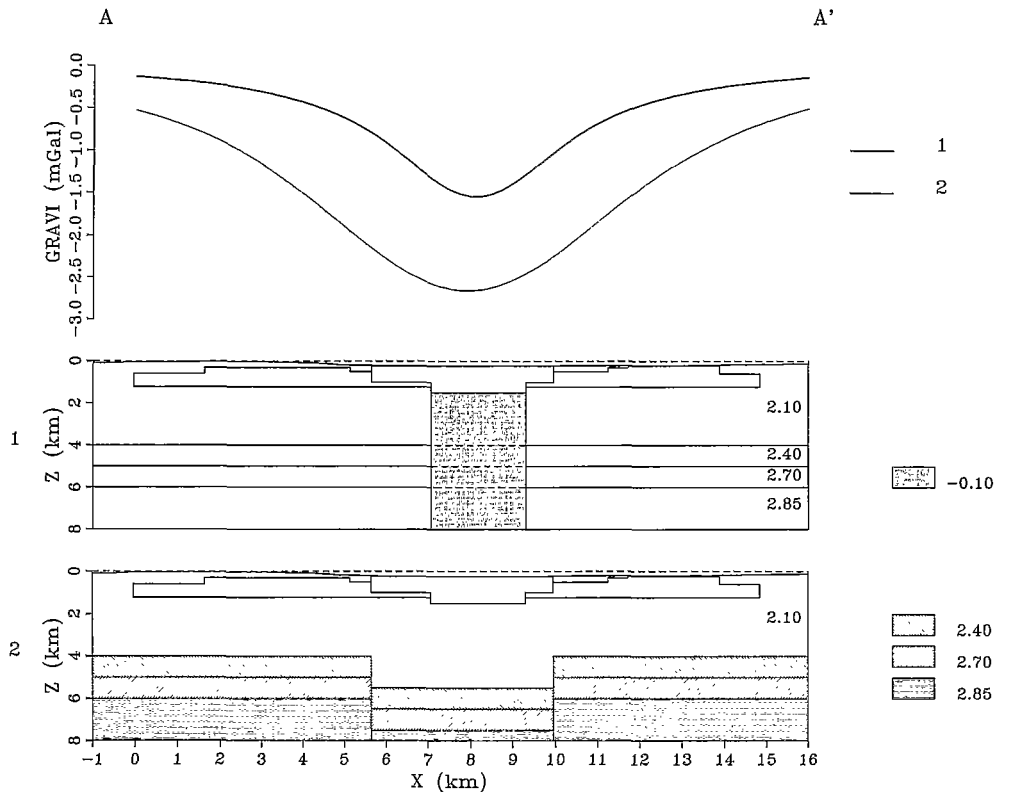

Fig. 16. Gravity effect of two different 3-D models for the deep structure below the Krakatau volcanic complex shown on a vertical section along line AA' (see location on Fig. 14). *Lower part*: Model 1 = model of caldera formation by 'chaotic' collapse; Model 2 = model of caldera formation by 'piston-type' collapse. In the two models, the collapsed roof of the magma chamber is supposed to lie at a depth greater than 8 km. The superficial structure is recalled with light lines. *Upper part*: Computed gravity effects in mGal for models 1 (heavy solid line) and 2 (light solid line).

Subsurface structure

The observed Bouguer anomaly over the Krakatau volcanic complex may be explained with a subsurface model including a low-density caldera infill and the dense volcanic substratum of the proto-Krakatau. In order to fit the steep gravity gradients observed, a sub-vertical contact associated with a density contrast of about 0.7 g/cm^3 has to be introduced. Examination of the Bouguer anomaly maps computed with various density values reveals that a density of 2.6 g/cm^3 minimizes the variations of the Bouguer anomaly along the positive ring. Such a value is similar to the one proposed for ancient volcanic products on other volcanoes such as Mount St. Helens (Williams and Finn, 1985) or the Toba caldera in the Sunda arc (Nishimura et al., 1984). So we choose 2.6 g/cm^3 for the density of the substratum of the proto-Krakatau. According to the total density contrast (0.7 g/cm^3) required for matching the steep gradients, we deduced a density of 1.9 g/cm^3 for the caldera infill. Due to this contrast and as no direct field observation on the nature and the density of these submarine materials are available, we suggest that they contain both juvenile pyroclastic products and older lithic rocks of the destructed island. The densities deduced from many studies for these volcanic materials usually range between 2.0 and 2.2 (Nishimura et al., 1984; Rymer et Brown, 1986; Alatorre-Zamura and Campos-Enriques, 1991; Zubin et al., 1992). Our value indicates that the average density of the filling-up materials tends towards low values for

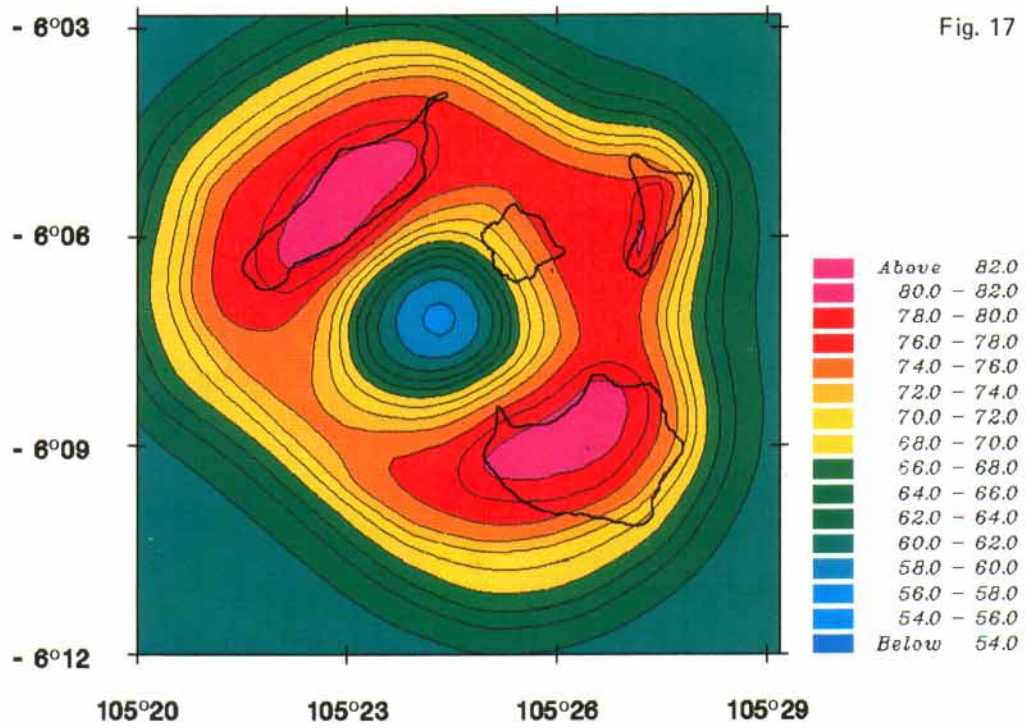
- 6°03
- 6°06
- 6°09
- 6°12
105°20
105°23
105°26
105°29
Above 82.0
80.0 – 82.0
78.0 – 80.0
76.0 – 78.0
74.0 – 76.0
72.0 – 74.0
70.0 – 72.0
68.0 – 70.0
66.0 – 68.0
64.0 – 66.0
62.0 – 64.0
60.0 – 62.0
58.0 – 60.0
56.0 – 58.0
54.0 – 56.0
Below 54.0

Fig. 17

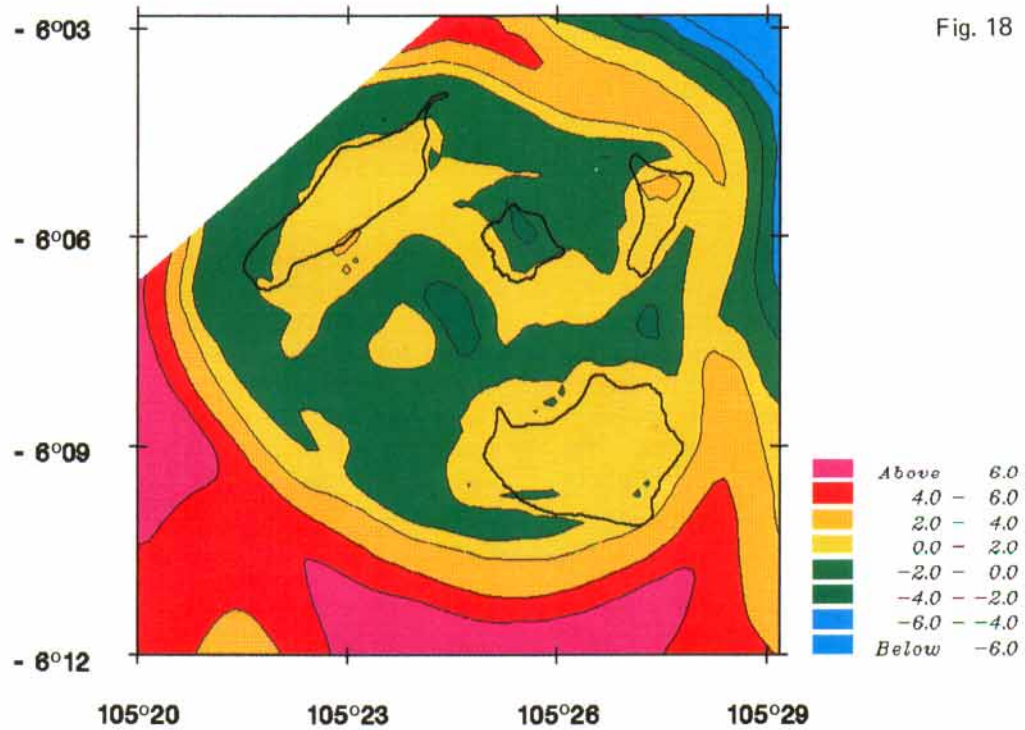
- 6°03
- 6°06
- 6°09
- 6°12
105°20
105°23
105°26
105°29
Above 6.0
4.0 – 6.0
2.0 – 4.0
0.0 – 2.0
−2.0 – 0.0
−4.0 – −2.0
−6.0 – −4.0
Below −6.0

Fig. 18

volcanic products. It might be explained by an homogeneous light infill or by an heterogeneous infill consisting of blocks or a combination of both sources.

Therefore, the density contrast with respect to our reference value of 2.1 g/cm^3 are about +0.5 g/cm^3 for the dense substratum and −0.2 g/cm^3 for the caldera infill. The geometry of our best-fit model is shown on Figs. 13 and 14. The substratum is sub-cylindrical with a hole in the centre. Its thickness is on average 1000 meters, its flat bottom lies at a depth of about 1225 m.b.s.l. and its top at 225 m.b.s.l. except beneath the outer islands where it forms their basement. As land data has been gathered mainly along the shores, detailed density model of the internal part of the outer islands would be poorly constrained. Therefore, the upper limit of the dense substratum lies arbitrarily at sea level. The middle depression is filled with up to 1000–1500 m of light material. Figure 15 shows three vertical sections across the density model along lines AA′, BB′ and CC′ (see location on Fig. 14) and the corresponding observed and computed gravity profiles. The fit between the observed anomaly and the computed one was considered as good if smaller than the accuracy of the observed Bouguer anomaly, that is 1 mGal for land data and 2.5 mGal for marine data, when close to the data points.

In this model, we interpret the origin of the positive anomalies as a dense substratum made of ancient magmatic rocks that form the basement of the outer islands. This is in good agreement with the hypothesis on the inner structure of the volcano made by Verbeek in 1885 on the basis of geological investigations. He proposed that the outer islands were built by accumulation of deposits from successive eruptions on the remnants of the proto-volcano. These ancient rocks form outcrops on some places of Rakata, Sertung and Panjang (see Fig. 2) and consist of 'trydimite andesite'. The comparison of the shape of the islands with the contour lines of the positive anomaly confirms that the southeastern part of Rakata and the north and northeastern part of Panjang are formed with younger volcanic products emplaced during recent eruptions.

Another hypothesis might be advocated in order to explain the origin of the positive anomaly. Density measurements were performed on pyroclastic rocks drilled in Campi Flegrei (Barberi et al., 1991) and have shown an increase of density with depth up to +0.2 g/cm^3 resulting from both compaction and hydrothermal circulation along circular faults. On the other hand, numerous well data obtained on a geothermal site in Costa-Rica (Miravalles volcano) did not show any increase of density due to hydrothermal effect (Hallinan et al., 1992). Although one cannot completely discard such an hypothesis for Krakatau, we favour the first hypothesis that is supported by geological data.

Deep structure

For the deepest part, we tested two different models, both compatible with the collapse of the top of a magma chamber. Scandone (1990) recently discussed various models of caldera formation. He suggested that the shape of the gravity anomaly allows to discriminate between piston-like or chaotic collapse. In the piston-like model, the collapse of the roof of the magma chamber is entirely transmitted up to the surface and results in the formation of a flat bottom caldera. Chaotic collapse is produced by the progressive breaking away of the rocks from the top of the magma chamber. A chimney, with a density lower than the original density, is then formed. Depending upon the size of the magma

Fig. 17. Computed gravity effect in mGal of our 3-D density model (shown on Figs. 13–15) over the whole area. A constant regional value of +62 mGal has been added to the computed gravity effect. This map is very close to the observed Bouguer anomaly map (Fig. 11).

Fig. 18. Residual map obtained by removing the computed effect of the 3-D density model (Fig. 17) from the observed Bouguer anomaly map (Fig. 11). The fit is better than 2 mGal (equivalent to the gravity data accuracy) over the volcanic complex where gravity data are available. Departures greater than 2 mGal occurred outside the complex where the gravity modelling is not constrained due to the lack of data.

chamber and the strength of the material, the chimney can reach the surface and create a funnel shape caldera. The corresponding gravity anomaly is negative for both models but the piston-like model anomaly presents a U-shape whereas the chaotic model anomaly is characterized by a V-shape. On this basis, Scandone (1990) suggested that the observed gravity anomalies over Krakatau, Aira (Japan), Campi Flegrei (Italy) and Santorini (Greece) better fit the chaotic model. But such a discrimination based on observed gravity gradients seems in fact difficult to evidence if the caldera is filled in with low-density material, which is the main source for the negative anomaly.

Figure 16 shows the two models tested. The first one is close to the chaotic model proposed by Scandone (1990) and thus is characterized by the presence of a chimney filled up with an heterogeneous material. This chimney extends from the top of the magma chamber to the bottom of the caldera infill. The density contrast for the material inside the chimney is taken as -0.1 g/cm^3 with respect to a reference crustal model. The second model is the piston-like subsidence of the crustal layers with an amplitude of 1500 meters, that is roughly the entire collapse of the caldera in our model (bathymetric depression plus infill). The reference density crustal model is deduced from velocities obtained by a refraction study close to Krakatau (Larue, 1983; Diament et al., 1990) using Birch's law (Nafe and Drake, 1963). The gravity effect for the two models is nearly identical with a maximum amplitude on the order of 2 mGal. According to our data distribution and precision, we cannot discriminate between both mechanisms. Nevertheless, as the wavelength of this effect is comparable to the one of the observed Bouguer anomaly, we have retained one of these two models in order to take into account this small contribution in our interpretative models shown on Fig. 15.

The gravity effect of the complete density model (subsurface plus chimney) was also computed on the whole area and is shown on Fig. 17. Wavelength and amplitude are comparable to the ones of the observed Bouguer anomaly map. A difference map (Fig. 18) confirms that close to the data points the misfits are smaller than 2 mGal.

7. Discussion

7.1. Extension with depth of the bathymetric depressions

Modelling of the observed Bouguer anomaly reveals the deep structure of the volcanic substratum and allows us to image the extension with depth of the bathymetric depressions. A collapsed zone within the substratum lies below the bathymetric depression characterized by a rectangular shape and a flat bottom, southwest of Anak (A on Fig. 7). On the contrary, the bathymetric depression located between Anak and Panjang (D) as well as the east–west trending graben north of Rakata (C) are not associated with any deep collapse (see Figs. 13, 14 and 15). Note however that our gravity map is better constrained on the E–W graben that between Anak and Panjang due to the data distribution (see Fig. 9). Nevertheless the observed gradients do not advocate for any important gravity low between Anak and Panjang islands. As for the narrow graben south of Sertung (B), it is associated to a small depression in the substratum of about 100 m (see Figs. 13, 14 and 15). It can be attributed both to a tectonic origin and/or to a horseshoe shape of the ancient volcano such as the one observed during the first stages of the growth of Anak by Sudrajat (1982).

Therefore, gravity data interpretation clearly points out that only the rectangular part of the bathymetric depression located SW of Anak (A on Fig. 7) is related to a deep cave-in of the volcanic substratum. In other words, the underground structure is much smaller in diameter than the present bathymetric outline of the morphological depression. Such a feature was also recognized in most Japanese calderas (Aramaki, 1984).

7.2. Shape of the substratum depression

The geometry of the substratum, as deduced from our model, is compatible with the emplace-

ment of one or several collapse caldera. To the centre of the model, the depression in the substratum has a funnel shape with two distinct slopes. The upper one is moderate and prolongs the inner parts of Rakata, Sertung and Panjang islands; it is covered with 2.1 g/cm^3 density material (Fig. 15b). Such a geometry might be interpreted as the result of one or more pre-historical collapses before the 1883 eruption. The deeper slope is larger and is located just below the flanks of the rectangular part of the bathymetric depression SW of Anak island; it limits the area filled up with a low density material (see Fig. 15b and 15c). Thus, the deep depression was probably formed during the 1883 eruption.

7.3. Location of the zone of maximum collapse with respect to the present magma bodies

It is noteworthy to compare the zone of maximum collapse in our model (Fig. 14) with the location of the magma chambers deduced from anomalous S waves (Fig. 3). It is located above a zone where no seismic attenuation has been reported, just between two magma bodies. This observation is consistent with a collapse of a part of the roof of a larger magma chamber during the 1883 eruption. Indeed, Vincent et al. (1989) already proposed that a large reservoir would have been separated in two magma pockets by the collapse of its central part. Comparison of gravity and seismological interpretations confirms this hypothesis.

7.4. Volumes of the 1883 eruption

Let us now compare the volume of the depression in the volcanic substratum, as given by our gravity modelling, with respect to the one of the erupted products of 1883. 3-D gravity modelling requires a low-density funnel-shaped body below the floor of the 1883 caldera. For Krakatau-type calderas, silicic caldera infill has been currently proposed and provide an adequate explanation (Rymer and Brown, 1986). Therefore, this infill has to be taken into account for the estimation of the volume of the erupted products. The difficulty arises with the amount of juvenile products within the depression. For Krakatau, we propose in this paper that this infill probably contains both juvenile products and shattered rock fragments of the destructed volcano. Indeed, the volume lost during the 1883 eruption (both above and below sea-level) has probably disappeared partly by engulfment and partly by gravitational failure, the debris lying either on the sea-bottom or in the infill. So, one can write that the proximal volume of the juvenile products plus the volume of the debris of the destructed volcano must be roughly equal to the volume of the deposits close to the volcanic complex plus the volume of the infill:

$$V_{\text{PProducts}} + V_{\text{Debris}} = V_{\text{Deposits}} + V_{\text{Infill}} \quad (4)$$

V_{Deposits} has been recently estimated by Sigurdsson et al. (1991a) as 13.6 km^3.

V_{Infill} is deduced from our 3-D model, 11.4 km^3. However, gravity modelling alone cannot provide a definitive value for this volume. The first uncertainty is related to the density contrast, a larger one yielding to a smaller volume. However, 1.9 g/cm^3 seems to be a lower limit for the mean density of the infill because even though it is composed of light products, its thickness results in some amount of compaction. For example, typical measured densities of the Cerro Galan (Argentina) ignimbrite within the caldera (1200 m thick) range between 2.1 and 2.4 g/cm^3 (Francis et al., 1983). A second uncertainty deals with its geometry itself: the horizontal extension is well constrained by the location of the observed gravity gradients but the depth of its base is not clearly resolved. Increasing this depth of a few hundred metres slightly affects the calculated anomaly simply because the further the sources, the smaller is the gravity effect. So, 11.4 km^3 has to be considered as a minimum value.

V_{Debris} is more difficult to estimate because debris might come both from the lost structure and the walls of the underground funnel-shaped structure. Moreover, according to the localisation of the funnel-shaped structure in the substratum with respect to the bathymetric depression and to the pre-1883 volcano, we propose that at most one half of the lost volume (i.e. 25 to

50%) has foundered *en masse* and that the other part has became fragments. So:

$V_{\text{Debris}} = A \cdot V_{\text{lost}} \cdot \rho_{\text{volcano}} / \rho_{\text{debris}}$ with $\frac{1}{2} < A < \frac{3}{4}$

The lost volume is roughly 5 km^3 above sea-level (Yokoyama, 1981) and 9 km^3 below sea-level (Sigurdsson et al., 1991a). Assuming 2.5 g/cm^3 and 1.9 g/cm^3 for the densities of the volcano and the debris respectively, V_{Debris} ranges between 9 and 13.5 km^3.

Therefore, he proximal volume for the erupted products becomes:

$V_{\text{PProducts}} = V_{\text{Deposits}} \pm 2.5 km^3 = 11\text{–}16 km^3$

that is in the range of previous estimations (Verbeek, 1885).

Following the estimation of Self and Rampino (1981) for the distal products (6–9 km^3), the volume of the total erupted products is then 17–25 km^3.

It is common to compare the volume of withdrawn magma with the lost volume. However, such a comparison is only valid in terms of orders of magnitude. In fact to equalize these two volumes requires first that all withdrawn magma is erupted. It requires also a piston-type collapse where the whole lost volume has settled down as a block. In that case one should find the topography of the volcano on the bottom of the caldera. This was observed after the formation of Fernandina caldera (Galapagos) in June 1868 where a cone has come down by 300 metres (Scandone, 1991). In most cases of Krakatau type calderas, the bottom of the caldera is flat and modelling of gravity data yields to underground funnel-shaped structures in which juvenile products and fragments of the destructed volcano accumulate. The initial volume of the destructed volcano should have been increased by fragmentation and the volume of collapse should be larger than the lost volume. Therefore in most cases, the volume of withdrawn magma should be larger than the lost volume.

Another difficulty arises when estimating the volume of magma. If all withdrawn magma is erupted, one can write:

$V_{\text{magma}} = V_{\text{Products}} \cdot \rho_{\text{products}} / \rho_{\text{magma}}$.

The value of this density ratio is poorly constrained but is commonly assumed to lie between 0.5 and 0.9. A mean ratio ranging between 0.7 and 0.8 is in good agreement with the density values used in our gravity modelling: assuming an initial density of the magma of 2.6 g/cm^3, the mean density of the products would be 1.9–2.1 g/cm^3.

Varying the density ratio between 0.7 and 0.8 yields $V_{\text{magma}} = 12\text{–}20 km^3$.

This value is slightly larger than previous estimations (9–10 km^3 from Self and Rampino, 1981) based on different assumptions. Nevertheless one must keep in mind that, due to the previously mentioned uncertainties, our estimations are only indicative.

The two important points to remind are:

(1) 3-D gravity interpretation requires a low-density body beneath the floor of the 1883 caldera and its volume has to be taken into account in the estimations of the erupted products.

(2) The location of the underground collapse with respect to the pre-1883 volcano implies that the lost volume should have disappeared both by engulfment and by gravitational failure, the debris lying either on the sea-bottom or in the infill.

7.5. Consequences for the scenario of the destruction of the pre-1883 volcano

The linear northeastern border of the deep depression in the substratum trends N150°E (Fig. 14). Its geometry is well constrained by the location of our gravity data on Anak. It follows the direction along which old and recent vents of Krakatau are distributed (dashed line on Fig. 2). Thus, gravity interpretation favours the existence of the postulated N150° tectonic weakness zone that could have guided both the development of the volcanic activity (vents of Danan, Perbuatan and Anak have successively took place along this line) and the caldera emplacement during the 1883 eruption. Clearly, this major weakness zone passing through the summit line of the pre-1883 Krakatau volcano must be introduced in the models of the 1883 eruption as a significant disruption surface of the volcanic edifice. Moreover, the southwards prolongation of

the N150° line intersects the Rakata coastline at its northern cape (see Fig. 2). To the west of this cape lies the spectacularly concave cliff extending up to the summit of the island along which most of the northern part of the cone would have slumped down; to the east, the shape of the coastline and of the topographic and bathymetric isolines (see Fig. 7) clearly image a smaller slumping cliff. Therefore, the missing part of the cone has probably slumped into the sea along two collapse zones located on each side of the N150° line!

Thus, in light of these new geophysical data, we propose that the western part of the volcano had preferentially foundered by engulfment at the time of the caldera collapse whereas the eastern part had slumped on the sea-bottom towards northern and eastern areas.

What triggered the collapse of the volcano? Collapse of the roof of the magma chamber does not occur necessarily at the end of the eruption sequence. As pointed out by Williams and McBirney (1979) and McBirney (1990), "*eruptions are not necessarily the cause of collapse; in many instances it is the collapse that has triggered the eruption rather than vice-versa* (McCall, 1963)". In the same way, Druitt and Sparks (1984) proposed that eruptions producing large volume of ignimbrite involve two well-defined stages. The first stage begins with an over-pressured magma that produces pumice-fall deposits. The authors show that only a small to moderate volume can be erupted during this stage. Then the pressure decreases to values less than lithostatic pressure. Initiation of the second stage is marked by the onset of the caldera collapse. Substantial volumes of magma can then be driven to the surface. In a generalised scheme of the evolution of a caldera-forming eruption, Scandone (1991) proposed also that collapse begins during or at the end of the plinian phase.

This model can be applied to the Krakatau 1883 eruption where the two stages have been recognized: a plinian phase followed by the extensive emission of ignimbrites. We propose that the roof of the magma chamber began to collapse at the end of the plinian phase along the N150° weakness zone. Movement along this zone probably weakened the volcanic edifice yielding to a slumping of its northeastern flank on the sea-bottom. The bathymetric depression located between Anak and Panjang (D on Fig. 7), which does not seem associated with any deep collapse, may result from the slumping of this part of the volcano, the debris lying further north and east. Indeed, hummocky sea-bottom topography has been observed there (Camus et al., 1992). The fact that the upper part of the hummocks consists of pyroclastic products (Sigurdsson, 1991a,b) is in good agreement with an avalanching of the northeastern flank of the old volcano before the eruption of ignimbrite.

This event, creating a sudden lowering of the lithostatic pressure on the vent, may be responsible for the onset of the generation of pyroclastic flows. Several units of pyroclastic flows have been identified on the islands deposits (Sigurdsson et al., 1991b). The caldera might have collapsed with successive phases related to these different episodes of magma draining. We propose that progressive collapse of the caldera and foundering of the western part of the volcano may have occurred throughout the stage of emission of ignimbrite. The presence of the low-density infill below the caldera favours this hypothesis. Finally, the northern face of Rakata slumped into the sea as previously described.

Camus and Vincent (1983a,b), Vincent and Camus (1986) and Camus et al. (1992) already proposed a flank failure of the volcano to explain the drastic change from plinian to ignimbritic activity. So we agree with them but our scenario differs on several points:

- only a small part of the volcano would have slumped into the sea and produced the debris avalanche before the emission of ignimbrite (the northeastern part and not all the missing structure).
- the initial desequilibrium would be produced along the N150° weakness zone and be related to the onset of the collapse of the roof of the magma chamber.
- the northern face of Rakata would have disappeared late in the eruption sequence as proposed by Francis and Self (1983).

Therefore, analysis of the morphology of the

Krakatau complex and gravity data modelling do not allow to discriminate between the two recent scenarios for the 1883 eruption (described in the Introduction part of this paper) but favour a 'mixed model' in which the western part of the former Krakatau island had preferentially foundered by engulfment at the time of the caldera collapse whereas the eastern part had slumped on the sea-bottom.

Acknowledgements

This study was financially supported by the "Délégation aux Risques Majeurs" and by INSU "Géosciences Marines". The authors are indebted to Professor M.T. Zen (BPPT, Jakarta) for providing a constant support in this French–Indonesian Research Program. We thank the captain, officers and the crew of the Indonesian R/V *Baruna Jaya III* and all the Indonesian and French scientists who participated to the Mentawai oceanographic cruise. The field operations would not have been possible without the efficiency of the geophysical team of Edy Arsadi (LIPI, Bandung). We thank our colleagues Yves Albouy, Gilbert Juste, Germinal Gabalda (ORSTOM, Bondy) and M.T. Zen Jr. (IPG, Paris) for their assistance in survey preparation and Dominique Rémy (ORSTOM, Bondy) for providing us the code for MNT representation. We benefited of discussions with R. Scandone, I. Yokoyama, P. Vincent and of comments on the manuscript by M. Semet, R. Scandone and an anonymous reviewer. IPGP contribution 1317.

References

Alatorre-Zamura, M.A. and Campos-Enriques, J.O., 1991. La Primavera Caldera (Mexico): Structure inferred from gravity and hydrogeological considerations. Geophysics, 56: 992–1002.

Aramaki, S., 1984. Formation of the Aira Caldera, southern Kyushu, ≈22 000 years ago. J. Geophys. Res., 89(B10): 8485–8501.

Barberi, F., Cassano, E., Torre, P.L. and Sbrana, A., 1991. Structural evolution of Campi Flegrei caldera in light of volcanological and geophysical data. J. Volcanol. Geotherm. Res., 48: 33–49.

Blake, S. and Ivey, G.N., 1986. Magma-mixing and the dynamics of withdrawal from stratified reservoirs. J. Volcanol. Geotherm. Res., 27: 153–178.

Brown, G.C., Rymer, H. and Thorpe, R.S., 1987. The evolution of andesite volcano structures: new evidence from gravity studies in Costa Rica. Earth Planet. Sci. Lett., 82: 323–334.

Budetta, G., Condarelli, D., Fytikas, M., Kolios, N., Pascale, G., Rapolla, A. and Pinna, E., 1984. Geophysical prospecting on the Santorini Islands. Bull. Volcanol., 47(3): 447–466.

Bulletin of the Global Volcanism Network, 1992. Smithsonian Institution, vol. 17, no. 10, 15 pp.

Camus, G. and Vincent, P.M., 1983a. Discussion of a new hypothesis for the Krakatau volcanic eruption in 1883. J. Volcanol. Geotherm. Res., 19: 167–173.

Camus, G. and Vincent, P.M., 1983b. Un siècle pour comprendre l'éruption du Krakatoa. La Recherche, 149: 1452–1457.

Camus, G., Gourgaud, A. and Vincent, P.M., 1987. Petrologic evolution of Krakatau (Indonesia): Implications for a future activity. J. Volcanol. Geotherm. Res., 33: 299–316.

Camus, G., Diament, M., Gloaguen, M., Provost, A. and Vincent, P.M., 1992. Emplacement of a debris avalanche during the 1883 eruption of Krakatau (Sunda Straits, Indonesia). Geojournal, 28(2): 123–128.

Chapman, M.E., 1979. Techniques for interpretation of geoid anomalies. J. Geophys. Res., 84(B8): 3793–3801.

Dahrin, D., 1993. Etude bathymétrique et gravimétrique du Détroit de la Sonde et du volcan Krakatau (Indonésie): Implications géodynamiques et volcanologiques. Thesis, Univ. Paris VII, 335 pp.

Diament, M., Deplus, C., Harjono, H., Larue, M., Lassal, O., Dubois, J. and Renard, V., 1990. Extension in the Sunda Strait (Indonesia): a review of the Krakatau programme. Oceanol. Acta, 10: 31–42.

Diament, M., Harjono, H., Arsadi, E., Bonvalot, S., Dahrin, D., Deplus, C., Dubois, J. and Zen Jr, M.T., 1991. A geophysical study of the Krakatau volcanic complex. EUG VI Strasbourg, Terra, 3(1): 266.

Druitt, T.H. and Sparks, R.S.J., 1984. On the formation of calderas during ignimbrite eruptions. Nature, 310: 679–681.

Effendi, A.C., Bronto, S. and Sukhyar, R., 1986. Geological map of Krakatau Volcanic Complex. Volcanological Survey of Indonesia.

Escher, R.G., 1919. De Krakatau groep als Vulkaan. Handel. Eerste Nederl. Ind. Natuurw. Congr., pp. 28–35.

Fedi, M., Nunziata, C. and Rapolla, A., 1991. The Campania–Campi Flegrei area: a contribution to discern the best structural model from gravity interpretation. J. Volcanol. Geotherm. Res., 48: 51–59.

Francis, P.W., 1985. The origin of the 1883 Krakatau tsunamis. J. Volcanol. Geotherm. Res., 25: 349–363.

Francis, P.W. and Self, S., 1983. The eruption of Krakatau. Sci. Am., 249: 146–159.

Francis, P.W., O'Callaghan, L., Kretzschmar, G.A., Thorpe, R.S., Sparks, R.S.J., Page, R.N., de Barrio, R.E., Gillou, G. and Gonzalez, O.E., 1983. The Cerro Galan ignimbrite. Nature, 301: 51–53.

Hallinan, S., Brown, G. and Rymer, H., 1992. Geophysical assistance in geothermal field assessment and monitoring, Miravalles, Costa-Rica. Final Rep. (ODA Ref. FNI 8788/541/093) Dep. Earth Sciences, The Open University, Milton Keynes, England, 211 pp.

Harjono, H., 1988. Géodynamique du Détroit de la Sonde (Indonésie): Apports des données de microsismicité et implications volcanologiques. Thesis, Univ. Paris-Sud, 262 pp.

Harjono, H., Diament, M., Nouaili, L. and Dubois, J., 1989. Detection of magma bodies beneath Krakatau volcano (Indonesia) from anomalous shear waves. J. Volcanol. Geotherm. Res., 39: 335–348.

Harjono, H., Diament, M., Dubois, J. and Larue, M., 1991. Seismicity of the Sunda Strait: evidence for crustal extension and volcanological implications. Tectonics, 10: 17–30.

Heiken, G. and Mc Coy, F., Jr, 1984. Caldera development during the Minoan eruption, Thira, Cyclades, Greece. J. Geophys. Res., 89(B10): 8441–8462.

Isherwood, W., 1976. Proc. 2nd U.N. Symposium on the Development and Use of Geothermal Resources. U.S. Government Printing Office, Washington D.C., 2: 1065–1073.

Iyer, H., 1984. Geophysical evidence for the locations, shapes and sizes, and internal structures of magma chambers beneath regions of Quaternary volcanism. Philos. Trans. R. Soc. London, Ser. A, 310: 473–510.

Judd, J.W., 1889. The earlier eruptions of Krakatau. Nature, 40: 365–366.

Kane, M.F., Mabey, D.R. and Brace, R.L., 1976. A gravity and magnetic investigation of the Long Valley Caldera, Mono County, California. J. Geophys. Res., 81: 754–762.

Larue, M., 1983. Corindon IX Cruise Report.

Lassal, O., Huchon, P. and Harjono, H., 1989. Extension crustale dans le Détroit de la Sonde (Indonésie). Données de la sismique réflexion (Campagne Krakatau). C.R. Acad. Sci. Paris, 309: 205–212.

Latter, J.H., 1981. Tsunamis of volcanic origin: summary of causes, with particular reference to Krakatau. Bull. Volcanol., 44: 467–490.

Longman, I.M., 1959. Formulas for computing the tidal acceleration due to the moon and the sun. J. Geophys. Res., 64: 2351–2355.

McBirney, A., 1990. An historical note on the origin of calderas. J. Volcanol. Geotherm. Res., 42: 303–306.

Nafe, J.E. and Drake, C.L., 1963. Physical properties of marine sediments. In: The Sea. McGraw-Hill, Wiley Inter-Sciences, London-New York, pp. 794–815.

Nettleton, L.L., 1976. Gravity and Magnetics in Oil Prospecting. Mc Graw-Hill, New York, NY.

Neumann van Padang, M., 1933. De Krakatau voorheen en thans. De Tropische Natuur, 22: 137–150.

Ninkovich, D., 1979. Distribution, age and chemical composition of tephra-layers in deep-sea sediments off Western Indonesia. J. Volcanol. Geotherm. Res., 5: 67–86.

Nishimura, S., Abe, E., Nishida, J., Yokoyama, T., Dharma, A., Hehanusa, P. and Hehuwat, F., 1984. A gravity and volcanostratigraphic interpretation of the Lake Toba Region, North Sumatra, Indonesia. Tectonophysics, 109: 253–272.

Nishimura, S., Nishida, J., Yokoyama, T. and Hehuwat, F., 1986. Neo-Tectonics of the Strait of Sunda, Indonesia. J. Southeast Asian Earth Sci., 1: 81–91.

Noujaim, A.K., 1976. Drilling in high temperature and overpressured area Sunda Straits, Indonesia. Proc. Indonesian Petroleum Association. Fifth Annu. Convention, pp. 211–214.

Oide, K., 1968. Geotectonic conditions for the formation of the Krakatau-type calderas in Japan. Pacific Geol., 1: 119–135.

Parasnis, 1962. Principles of Applied Geophysics. Methuen, London, 176 pp.

Patella, D., 1988. An unambiguous derivation of the Bouguer gravity anomaly. Boll. Geof. Teor. Appl., 30(119-120): 345–352.

Rymer, H. and Brown, G.C., 1986. Gravity fields and the interpretation of volcanic structures: Geological discrimination and temporal evolution. J. Volcanol. Geotherm. Res., 27: 229–254.

Scandone, R., 1990. Chaotic collapse of calderas. J. Volcanol. Geotherm. Res., 42: 285–302.

Scandone, R., 1991. A reply to the comments by Yokoyama and De la Cruz-Reyna and some other ideas on the collapse of calderas and the generation of ignimbrites. J. Volcanol. Geotherm. Res., 47: 352–357.

Scandone, R., Bellucci, F., Lirer, L. and Rolandi, G., 1991. The structure of the Campanian Plain and the activity of the Neapolitan volcanoes (Italy). J. Volcanol. Geotherm. Res., 48: 1–31.

Self, S. and Rampino, M.R., 1981. The 1883 eruption of Krakatau. Nature, 294: 699–704.

Self, S. and Rampino, M.R., 1982. Comments on "A Geophysical interpretation of the 1883 Krakatau eruption" by I. Yokoyama. J. Volcanol. Geotherm. Res., 13: 379–386.

Sigurdsson, H., Carey, S., Mandeville, C. and Bronto, S., 1991a. Pyroclastic flows of the 1883 Krakatau eruption. EOS Trans. Am. Geophys. Union, 72: 377.

Sigurdsson, H., Carey, S. and Mandeville, C., 1991b. Submarine pyroclastic flows of the 1883 eruption of the Krakatau Volcano. National Geographic Research and Exploration, 7: 310–327.

Simkin, T. and Fiske, R.S., 1983. Krakatau 1883: The Volcanic Eruption and its Effects. Smithsonian Inst. Press, Washington, D.C., 464 pp.

Stehn, C.E., 1929. The geology and volcanism of the Krakatau Group. Proc. Fourth Pacific Sci. Congress (Batavia), pp. 1–55.

Sudrajat, A., 1982. The morphological development of Anak

Krakatau Volcano, Sunda Strait. Geol. Indonesia, 9: 1–11.

van Bemmelen, R.W., 1941. Krakatau. Bull. East Indian Volcanol. Surv., 18: 53–60.

Verbeek, R.D.M., 1885. Krakatau. In: T. Simkin and R.S. Fiske (Editors), Krakatau 1883 : the volcanic eruption and its effects. Smithsonian Inst. Press, Washington, D.C., pp. 169–277.

Vincent, P.M. and Camus, G., 1986. The origin of the 1883 Krakatau tsunamis, by P.W. Francis. Discussion. J. Volcanol. Geotherm. Res., 30: 169–177.

Vincent, P.M., Camus, G. and Gourgaud, A., 1989. Hypothèse sur la structure du Krakatau. Bull. Sect. Volcanol. Soc. Géol. France, 13.

Volcanological Survey of Indonesia, 1982. Bathymetric map (Escher, 1919) and topographic map (1979) of Krakatau volcanic complex.

Williams, D.L. and Finn, C., 1985. Analysis of gravity data in volcanic terrain and gravity anomalies and subvolcanic intrusions in the Cascade Range, USA, and at other selected volcanoes. In: W.J. Hinze (Editor), The Utility of Regional Gravity and Magnetic Anomaly Maps. Society of Exploration Geophysicists, Tulsa, OK, pp. 361–376.

Williams, H., 1941. Calderas and their origin. Bull. Dept. Geol. Sci., Univ. Calif., 25: 239–346.

Williams, H. and McBirney, A.R., 1979. Volcanology. Freeman, Cooper and Co, San Francisco, CA, 397 pp.

Yokoyama, I., 1981. A Geophysical interpretation of the 1883 Krakatau eruption. J. Volcanol. Geotherm. Res., 9: 359–378.

Yokoyama, I., 1987. A scenario of the 1883 Krakatau Tsunami. J. Volcanol. Geotherm. Res., 34: 123–132.

Yokoyama, I. and Hadikusumo, D., 1969. Volcanological survey of Indonesian volcanoes. Part 3: A gravity survey on the Krakatau Islands, Indonesia. Bull. Earthq. Res. Inst., 47: 991–1001.

Zen, M.T. and Sudradjat, A., 1983. History of the Krakatau volcanic complex in Strait Sunda and the mitigation of its future hazards. Bul. Jurusan Geol., 10: 1–28.

Zubin, M.I., Kozikev, A.I. and Luchitskiy, A.I., 1992. A gravitationally derived model of Klyuchevskoi Volcano, Kamchatka. Volcanol. Seismol., 12: 628–646.